

Network Induced Large Correlation Matrix Estimation

Shuo Chen^{1*}, Jian Kang², Yishi Xing¹, Yunpeng Zhao³, and Donald Milton⁴

¹ Department of Epidemiology and Biostatistics, University of Maryland, College Park, MD 20742, USA

² Department of Biostatistics, University of Michigan, Ann Arbor, MI 48109, USA

³ Department. of Statistics, George Mason University, Fairfax, VA 22030, USA

⁴ Maryland Institute for Applied Environmental Health, University of Maryland, College Park, MD 20742, USA

Abstract

The correlation matrix of massive biomedical data (e.g. gene expression or neuroimaging data) often exhibits a complex and organized, yet latent graph topological structure. We propose a two step procedure that first detects the latent graph topology with parsimony from the sample correlation matrix and then regularizes the correlation matrix by leveraging the detected graph topological information. We show that the graph topological information guided thresholding can reduce false positive and false negative rates simultaneously because it allows edges to borrow strengths from each other precisely. Several examples illustrate that the parsimoniously detected latent graph topological structures may reveal underlying biological networks and guide correlation matrix estimation.

Keywords: graph, large correlation matrix, network, parsimony, shrinkage, thresholding, topology.

1 Introduction

We consider a large data set $\mathbf{X}_{n \times p}$ with the sample size n and the feature dimensionality of p . The estimation of the covariance matrix $\mathbf{\Sigma}$ or correlation matrix \mathbf{R} is fundamental to understand the

*Correspondence to: shuochen@umd.edu

inter-relationship between variables of the large data set $\mathbf{X}_{n \times p}$ (Fan *et al*, 2015).

Various regularization methods have been developed to estimate the high-dimensional covariance matrix. For instance, ℓ_1 the penalized maximum likelihood has been utilized to estimate the sparse precision matrix $\Theta = \Sigma^{-1}$ (Friedman *et al*, 2008; Banerjee *et al*, 2008; Yuan and Lin, 2007; Lam and Fan, 2009; Yuan, 2010; Cai and Liu, 2011; Shen *et al*, 2012). In addition, the covariance matrix thresholding methods have been developed to directly regularize the sample covariance matrix (Bickel and Levina, 08; Rothman *et al*, 2009; Cai *et al*, 2011; Zhang, 2010; Fan *et al*, 2013; Liu *et al*, 2014). Similarly, the thresholding regularization techniques have also been applied to correlation matrix \mathbf{R} estimation (Qi and Sun, 2006; Liu *et al*, 2014; Cui *et al*, 2016). Mazumder and Hastie (2012) and Witten *et al* (2011) point out that the two sets of methods are naturally linked regarding vertex-partition of the whole graph and estimate of the graph edge skeleton.

Graph notations and definitions are often used to describe the relationship between the p variables of $\mathbf{X}_{n \times p}$ (Yuan and Lin, 2007; Mazumder and Hastie, 2012). A finite undirected graph $G = \{V, E\}$ consists two sets, where the vertex set V represents the variables $\mathbf{X} = (X_1, \dots, X_p)$ with $|V| = p$ and the edge set E denotes relationships between the vertices. Let $e_{i,j}$ be the edge between nodes i and j . Then $e_{i,j}$ is an connected edge if nodes i and j are genuinely correlated in G . Under the sparsity assumption, the regularization algorithms assign most edges as unconnected, and G may be decomposed to a set of maximal connected subgraphs (Witten *et al*, 2011; Mazumder and Hastie, 2012).

Many recent works estimate the covariance matrix by taking the graph topological structure into account. For example, Witten *et al* (2011), Hsieh *et al* (2012), Tan *et al* (2015) utilize the diagonal block structure and Bien *et al* (2016) use the *banding* structure to improve the estimation of the covariance matrix. In many biomedical high-dimensional data sets, we find interactions between biological features (e.g. genes or neural processing units) often exhibit an interesting organized network graph topological pattern which consists a number of block/community subgraphs and a large random subgraph (see Figure 1). In this paper we develop a two step procedure that 1) first detects the graph topological structure *parsimoniously* and 2) then estimates the correlation matrix by leveraging the information of this graph topological structure.

Motivated by multiple practical biomedical large data analyses, we consider a graph topological structure as $G = G^1 \cup G^0$ where the subgraph $G^1 = \cup_{c=1}^{C_1} G_c$ is a stochastic block model structure and $G^0 = \cup_{c=1}^{C_0} G_c^0$ (G_c^0 is a singleton only consisting one node) can be considered as an Erdős-Rényi random graph (i.e. G is a mixture model and we refer it as the $G^1 \cup G^0$ mixture model). Thus, the $G^1 \cup G^0$ mixture model is a special case of the stochastic block model, which contains many singletons and a number of communities (Bickel and Chen, 2009; Karrer and Newman, 2011; Zhao *et al*, 2011; Choi *et al*, 2012; Nadakuditi and Newman, 2012; Lei and Rinaldo, 2014). However, the data sets are often noisy and thus the conventional clustering algorithms can not easily identify such structures (Tan *et al*, 2015). Therefore, we propose a new parsimonious algorithm to effectively estimate the $G^1 \cup G^0$ mixture structure, which is robust to false positive noises (edges). Our new approach impose an penalty term on the size of edges all $\{G_c\}$ such that include most highly correlated edges in communities of G^1 in communities with the minimum sizes of edges. That the new penalty term reduce the impact noises on the community estimation is due to the fact that the (sample) false positive highly correlated edges are often distributed in a random pattern rather in a community structure.

In step two, we estimate the large correlation by using the detected $G^1 \cup G^0$ mixture model graph topological structure. Specifically, we perform thresholding for edges within and outside communities adaptively by using Bayes factors, and thus detected graph topology serves as prior knowledge. In this way, the decision of thresholding an edge is made upon considering both this edge’s magnitude and the its *neighborhood* via the detected graph topological information. Therefore, our network based thresholding strategy allows edges to borrow strength from each other while avoiding the the computationally difficult step of estimation of the *covariance of edges* (i.e. correlation of correlations). Different from methods of Hsieh *et al* (2012) and Tan *et al* (2015) which mainly focus on the edges within block components, we utilize information of edges from both inside and outside diagonal blocks. We name the whole graph topology information guided regularization strategy **Network Induced Correlation matrix Estimation (NICE)**.

The NICE method makes three contributions: i) we propose a new penalized objective function that is well-suited to estimate latent graph topological structures and very robust to false positive

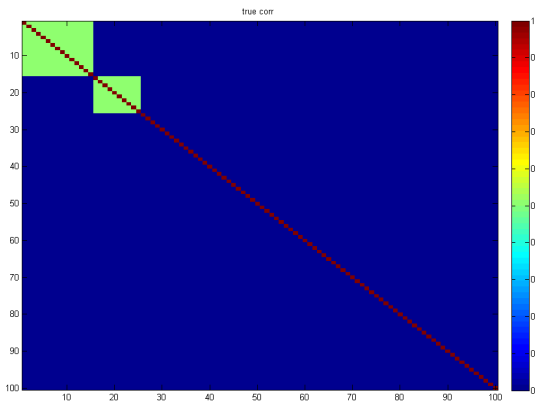
noises and we develop efficient algorithms to solve the objective function; ii) we fuse the graph topological information and thresholding decision making procedure to simultaneously reduce false positive and false negative discovery rates; iii) new statistical theories are developed. In addition, the detected topological structures not only assist to estimate the dependency relationship between each pair of variables, but also can reveal interesting underlying biological networks.

The paper is organized as follows. Section 2 describes the NICE algorithm, followed by theoretical results in Section 3. In Sections 4, we perform the simulation studies and model evaluation/comparisons and we apply our method to a mass spectrometry proteomics data set. Concluding remarks are summarized in Section 5.

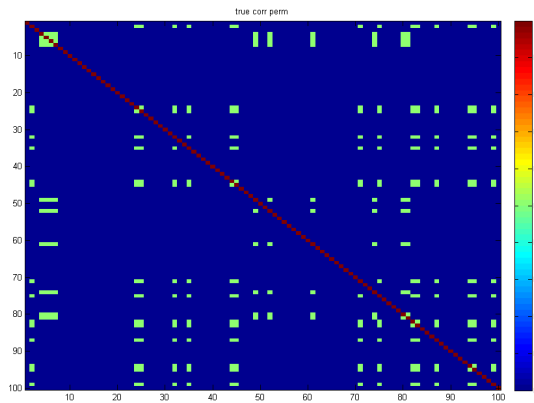
2 Methods

We consider the sample covariance \mathbf{S} and sample correlation matrix $\widehat{\mathbf{R}} = \text{diag}(\mathbf{S})^{-1/2} \mathbf{S} \text{diag}(\mathbf{S})^{-1/2}$ as our input data (Qi and Sun, 2006; Liu *et al*, 2014; Fan *et al*, 2015). We may directly perform hard thresholding on the sample correlation matrix to estimate \mathbf{R} by using $R_{i,j}^T = \{\widehat{R}_{i,j} I(|\widehat{R}_{i,j}| > T)\}$ without understanding the underlying network structure, where T is a pre-specified or calculated threshold. However, applying the universal regularization rule (even when optimal T is provided) to each element (or column) may introduce numerous false positives and false negatives due to various noises from the sample data. Therefore, we propose to leverage the information from the latent topological structure of the correlation matrix (i.e. graph G) to assist the decision making process.

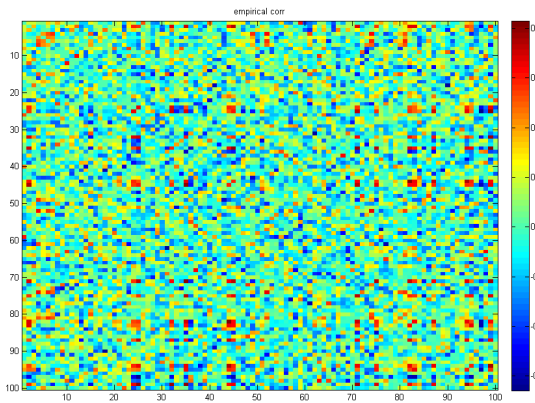
The NICE method consists two steps: i) we first detect the latent topological structure of $G = G^1 \cup G^0$ mixture in G by applying the rule of parsimony ii) we then apply empirical Bayes based thresholding to the sample correlation matrix guided by the detected graph topology.



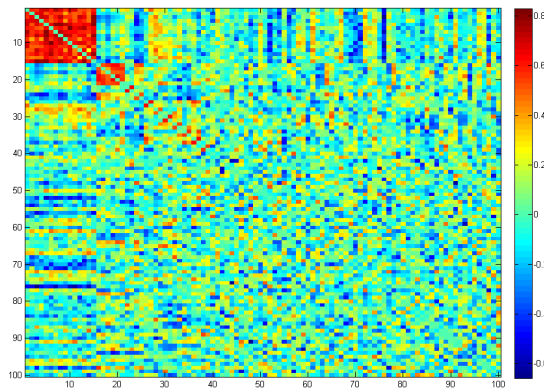
(a) The truth: two networks



(b) Shuffling the order of nodes



(c) The input data for NICE



(d) Network detection results

Figure 1: An example of a network induced covariance matrix: $|V|=100$ nodes and $|E|=4950$ edges, there are two networks (a) and in practice they are implicit (b) especially hard to recognize when looking at the sample covariance matrix (c); however, with the knowledge/estimation of topological network structures detected by NICE (d) the regularization strategy should take them into account.

2.1 Parsimonious estimation of latent networks from sample correlation matrix

We first define the weight matrix \mathbf{W} based on the empirically estimated correlation matrix $\widehat{\mathbf{R}}$. An entry $w_{i,j}$ of \mathbf{W} can be a transformed correlation coefficient between variables i and j that corresponds to the edge $e_{i,j}$ in G , for example, Fisher's Z transformation. $w_{i,j}$ is often a continuous metric. In Appendix, we describe an empirical Bayes based procedure to calculate $w_{i,j}$ as a metric between 0 and 1. \mathbf{W} is only used for the latent network detection rather than the regularization step.

We assume that G includes induced complete subgraphs (community networks) as shown in Figure 1a, the edges within the networks are more likely to be connected than edges outside networks. However, in practice this topological structure is latent. The sample correlation matrix has no explicit graph topological structure (1c). By optimizing the objective function 1 we can recognize the latent graph topological structures (1d). Next, we perform permutation tests to evaluate the statistical significance of each G_c , and the statistically significant subgraphs $\{G_c\}$ will be used to assist the estimation of the correlation matrix in the following step.

We aim to identify the latent $G^1 \cup G^0$ mixture structure from \mathbf{W} by using penalized optimization. The heuristic is to identify a set of subgraphs $U = \cup_{c=1}^C G_c$ that maximizes the sum of weights of edges in the union set with minimum subgraph sizes. The penalty term is used to avoid misrecognizing the network structure due to false positive noises. Formally, we propose an objective function

$$\arg \max_{C, \{G_c\}} \sum_{c=1}^C \exp\{\log(\sum (w_{i,j} | e_{i,j} \in G_c)) - \lambda_0 \log(|E_c|)\}, \quad (1)$$

with following definitions and conditions:

1. G_c ($c = 1, \dots, C$) is a clique subgraph that $G_c = \{V_c, E_c\}$ and $|V_c| \geq 1$;
2. the size of the a subgraph G_c is determined by the number of edges $|G_c| = |E_c|$;
3. $\cup_{c=1}^C V_c = V$, $\cap_{c=1}^C V_c = \emptyset$ and $\cup_{c=1}^C E_c \subseteq E$.

The objective function is non-convex and difficult to be directly solved. We develop iterative algorithm to optimize C and $\{G_c\}$. In Appendix, we provide the detailed derivation and optimization algorithms (including choosing the tuning parameter λ_0), which links 1 to a spectral clustering related objective function (von Luxburg, 2007; Nadakuditi and Newman, 2012). The number of subgrphs C is considered to be related to the penalty because $C = 1$ leads to $\cup_{c=1}^C E_c = E$ and $C = |V|$ indicates $\cup_{c=1}^C E_c = \emptyset$. Because of the penalty term, the objective function often selects a relatively large \hat{C} value and include many G_c as singletons by graph size shrinkage. The objective function is well-suited to capture topological structure from sample correlation matrix while being less affected by the false positive noises by implementing the new penalty term.

Therefore, implementing optimization to 1 yields estimates of the network topological structure underlying within the large correlation matrix, which can be used to guide the decision making procedure of correlation matrix thrsholding.

2.2 Graph topology oriented correlation matrix threshohlding

To estimate the correlation matrix \mathbf{R} , we perform graph topology guided thresholding on the sample correlation matrix $\hat{\mathbf{R}}$ by using Bayes factors. Let $z_{i,j}$ be the Fisher's Z transformed sample correlation coefficient of $\hat{R}_{i,j}$ and it follows a mixture distribution that $z_{i,j} \sim \pi_0 f_0(z_{i,j}) + \pi_1 f_1(z_{i,j})$.

Universal thresholding

Without considering prior information of the topology structure, the universal thresholding can be applied(Bickel and Levina, 08). For instance, an empirical Bayes framework implements a Bayes factor based via the (Efron, 2004, Schäfer and Strimmer, 2005). The hard-thresholding rule is often employed for this purpose (Cai *et al*, 2011, Fan *et al*, 2015), which sets an edge to zero unless

$$\frac{P(\delta_{i,j} = 1|z_{i,j})}{P(\delta_{i,j} = 0|z_{i,j})} = \frac{f_1(z_{i,j})\pi_1}{f_0(z_{i,j})\pi_0} \geq T,$$

T is a constant that is linked to local fdr cutoff, and π_0 and π_1 are the proportions of null and non-null distributions correspondingly. For example, $T = 4$ is equivalent to the cutoff of local fdr

of 0.2 (Efron, 2007). For instance, given $\pi_0 = 0.9$ and $\pi_1 = 0.1$, the universal decision rule is that an edge is thresholded when $\text{BF} = \frac{f_1(z_{i,j})}{f_0(z_{i,j})} \leq 36$. In practice, π_0 and π_1 are estimated based on the distribution of the statistics (e.g. $z_{i,j}$) and the Bayes factor cut-off is updated accordingly.

It has been well documented that the Bayes factor inferential models could adjust the multiplicity by adjusting the prior structure (Jeffreys, 1961; Kass and Raftery, 1995; Scott and Berger, 2006; Efron, 2007; Scott and Berger, 2010). The prior odds are tuned to control false positive rates, and a larger π_0 ($\pi_0 \rightarrow 1$) or a distribution of π_0 with larger mean leads to more stringent adjustment that may cause both low false positive discovery rates and high false negative discovery rates. Scott and Berger, 2006 suggest a prior distribution with median value around 0.9 and Efron, 2007 estimates π_0 by using an empirical Bayes model.

However, there has been a long term challenge for all universal regularization methods (e.g. shrinkage or thresholding): the trade-off between false positive and false negative findings. Moreover, edges may be dependent on each other in an organized topological pattern and the mass univariate edge inference (universal regularization) ignoring the dependency structure may not estimate the large covariance and correlation matrix effectively and efficiently. Yet, the direct estimation of the dependency structure between edges is challenging and sometimes not feasible. We propose one possible solution by leveraging latent graph topology to guide thresholding and account for the *dependency* between edges. The detected topological structure can seamlessly fuse into the empirical Bayes thresholding framework as prior knowledge and provides precise neighborhood information that allows edges to borrow strengths for each other.

Network based thresholding

In a network induced correlation matrix, an edge with sample correlation value $z_{i,j}$ is more likely to be truly connected within than outside a network community because the within community ‘neighbor’ edges are more connected. Thus, we incorporate the topological location information of an edge into the regularization procedure. We first calculate the prior odds (of being truly connected) for edges within and outside community networks separately by:

$$\theta_{in} = \frac{P(\delta_{i,j} = 0 | e_{i,j} \in G_c, \forall c)}{P(\delta_{i,j} = 1 | e_{i,j} \in G_c, \forall c)} = \frac{\pi_0^{in}}{\pi_1^{in}},$$

$$\theta_{out} = \frac{P(\delta_{i,j} = 0 | e_{i,j} \notin G_c, \forall c)}{P(\delta_{i,j} = 1 | e_{i,j} \notin G_c, \forall c)} = \frac{\pi_0^{out}}{\pi_1^{out}},$$

Clearly, the within community edges are more connected by and thus $\pi_1^{in} > \pi_1 > \pi_1^{out}$ and $\pi_0^{out} > \pi_0 > \pi_0^{in}$, and $\theta_{out} \geq \theta_{all} \geq \theta_{in}$.

Let edges inside and outside of the detected communities follow different distributions:

$$z_{i,j} | e_{i,j} \in G_c \sim \pi_0^{in} f_0(z_{i,j}) + \pi_1^{in} f_1(z_{i,j});$$

$$z_{i,j} | e_{i,j} \notin G_c \sim \pi_0^{out} f_0(z_{i,j}) + \pi_1^{out} f_1(z_{i,j}).$$

The proportions are different for inside and outside network, and overall edges, yet we assume that the null $f_0(z_{i,j})$ and non-null $f_1(z_{i,j})$ distributions are identical. By using the identified the latent community networks where edges are more correlated in step one, we propose the network based thresholding rule:

If $e_{i,j} \in G_c$,

$$\widehat{R}_{i,j}^{\mathcal{T}} = \begin{cases} \widehat{R}_{i,j} & \text{if } BF_{i,j} = \frac{\hat{f}_1(z_{i,j})}{\hat{f}_0(z_{i,j})} \geq T \cdot \hat{\theta}_{in}; \\ 0 & \text{otherwise.} \end{cases}$$

else if $e_{i,j} \notin G_c$,

$$\widehat{R}_{i,j}^{\mathcal{T}} = \begin{cases} \widehat{R}_{i,j} & \text{if } BF_{i,j} = \frac{\hat{f}_1(z_{i,j})}{\hat{f}_0(z_{i,j})} \geq T \cdot \hat{\theta}_{out}; \\ 0 & \text{otherwise.} \end{cases}$$

Equivalently, the we provide estimate of the edge set \widehat{E} by using:

$$\begin{aligned}\widehat{\delta}_{i,j}^{0,in} &= I \left(\frac{\widehat{f}_1(z_{i,j})}{\widehat{f}_0(z_{i,j})} \geq T \cdot \widehat{\theta}_{in} \right) \\ \widehat{\delta}_{i,j}^{0,out} &= I \left(\frac{\widehat{f}_1(z_{i,j})}{\widehat{f}_0(z_{i,j})} \geq T \cdot \widehat{\theta}_{out} \right),\end{aligned}\tag{2}$$

where $\delta_{i,j}^0$ is an indicator variable that $\delta_{i,j}^0 = 1$ when variables i and j are correlated with each other, otherwise $\delta_{i,j}^0 = 0$.

The detected graph topology provides the prior knowledge of the ‘neighborhood’ and ‘location’ of an edge, which accordingly allow graph topology guided thresholding while accounting for dependency between edges. A community network is analogous to a neighborhood (spatial closeness) of *edges* with explicit boundaries and edges within the neighborhood could borrow power from each other. Many statistical models are developed based on this idea, for example, the Ising prior and conditional autoregressive (CAR) model (Besag and Kooperberg, 1995). Nevertheless, unlike data in spatial or imaging statistics the sample correlation/covariance matrix of large biomedical data sets often include no available information about the exact spatial location or closeness. Thus, our detected graph topological structure provides a new pathway of regularization/statistical inferences on ‘edges’ by accounting for the dependency structure based on (detected) latent graph topological ‘closeness’.

We empirically estimate $\widehat{\theta}_{in}$ and $\widehat{\theta}_{out}$ from the data. First, let all edges that are Fisher’s Z transformed sample correlation coefficients in $\widehat{\mathbf{R}}$ follow a mixture distribution $f(z_{i,j}) = \pi_0^{all} f_0(z_{i,j}) + \pi_1^{all} f_1(z_{i,j})$. We estimate $\widehat{\pi}_0^{all}, \widehat{\pi}_1^{all}, \widehat{f}_0, \widehat{f}_1$ similarly to local *fdr* by algorithms used in (Efron, 2004). Next, we estimate $\widehat{\pi}_0^{in}$ for in-network edges $e_{i,j} \in G_c$. Since $\widehat{f}_0, \widehat{f}_1$ are estimated in the previous step, the only parameter to estimate in $f^{in}(z_{i,j}) = \pi_0^{in} f_0(z_{i,j}) + \pi_1^{in} f_1(z_{i,j})$ is $\widehat{\pi}_0^{in} = 1 - \widehat{\pi}_1^{in}$. We simply implement the maximum likelihood estimation and then obtain $\widehat{\theta}_{in} = \widehat{\pi}_0^{in} / \widehat{\pi}_1^{in}$. For edges outside of networks ($z_{i,j}$ that $e_{i,j} \notin G_c$) $f^{out}(z_{i,j}) = \pi_0^{out} f_0(z_{i,j}) + \pi_1^{out} f_1(z_{i,j})$ we estimate $\widehat{\pi}_0^{out}$ and calculate $\widehat{\theta}_{out} = \widehat{\pi}_0^{out} / \widehat{\pi}_1^{out}$ by following the same procedure. In general, our graph topological structure detection algorithm produces a very small odds ratio $\widehat{\theta}^{in} / \widehat{\theta}^{out}$ when the informative edges are distributed

in an organized pattern. Thus, the choice of T has a small impact on the decision making process. Uncovering graph topological structure is important to understanding the interactive relationships between multivariate variables (nodes) and the dependency between edges. We show that the detected topological structure can also provide prior knowledge to assist large covariance/correlation matrix regularization and estimation. The network based regularization approach utilizes the additional yet latent graph structure information and reduces false positive and negative discovery rates simultaneously (shown in section 4). We summarize the NICE algorithm of both steps in Algorithm 1 in the Appendix.

3 Theoretical Results

We start with some notations for the theoretical development. Let $X_{i,k}$ be the observed data on node i for subject k , for $i = 1, \dots, p_n$ and $k = 1, \dots, n$ with mean zero and unit standard deviation. Recall that $\mathbf{R} = \{R_{i,j}\}$ is the true correlation matrix of interests with $\text{Cor}(X_{i,k}, X_{j,k}) = R_{i,j}$ and $\widehat{\mathbf{R}} = \{\widehat{R}_{i,j}\}$ be the correlation matrix estimator. Let $\text{Fis}(x) = \log \{(1+x)/(1-x)\} / 2$ be the Fisher's Z transformation. Let $z_{i,j} = \text{Fis}(\widehat{R}_{i,j})$ and $\mu_{i,j} = \text{Fis}(R_{i,j})$, and $R_{i,j} = 0$ if and only if $\mu_{i,j} = 0$. Let $f_{i,j}(\cdot)$ be the density function of $z_{i,j}$. Let $\phi(x) = \exp(-x^2/2)/\sqrt{2\pi}$ be the standard normal probability density function. Let $\delta_{i,j}^0 = I[R_{i,j} \neq 0] = I[\mu_{i,j} \neq 0] = I[e_{i,j} \in G]$ indicate whether or not $e_{i,j} \in G$. Let $q_n = \sum_{1 \leq i < j \leq p_n} \delta_{i,j}^0$,

$$f_0(z) = \frac{\sum_{i < j} (1 - \delta_{i,j}^0) f_{i,j}(z)}{\sum_{i < j} (1 - \delta_{i,j}^0)}, \quad \text{and} \quad f_1(z) = \frac{\sum_{i < j} \delta_{i,j}^0 f_{i,j}(z)}{\sum_{i < j} \delta_{i,j}^0}.$$

Let $f(z)$ denote the actual distribution of $\{z_{i,j}\}_{1 \leq i < j \leq p_n}$.

$$f(z) = \pi_0 f_0(z) + \pi_1 f_1(z),$$

where

$$\pi_0 = \frac{p_n(p_n - 1) - q_n}{p_n(p_n - 1)} \quad \text{and} \quad \pi_1 = 1 - \pi_0.$$

Given data $\{z_{i,j}\}_{i < j}$, suppose $\widehat{f}_c(\cdot)$ be an estimator for $f_c(\cdot)$ for $k = 0, 1$, and $\widehat{\pi}_0$ is an estimator for π_0 with $\widehat{\pi}_1 = 1 - \widehat{\pi}_0$. For any $T > 0$ and $\widehat{\mathbf{R}}$, define the NICE thresholding operator $\text{NICE}(\widehat{\mathbf{R}}; T) = \{\text{NICE}(\widehat{R}_{i,j}; T)\}_{i < j}$. Specifically,

$$\text{NICE}(\widehat{R}_{i,j}; T) = \begin{cases} \widehat{R}_{i,j}, & \frac{\widehat{f}_1(z_{i,j})}{\widehat{f}_0(z_{i,j})} > \frac{\widehat{\pi}_0}{\widehat{\pi}_1} T, \\ 0 & \frac{\widehat{f}_1(z_{i,j})}{\widehat{f}_0(z_{i,j})} \leq \frac{\widehat{\pi}_0}{\widehat{\pi}_1} T. \end{cases}$$

3.1 Conditions

The following conditions are needed to facilitate the technical details, although they may not be the weakest conditions.

Condition 3.1. *We consider the following conditions on the data $\mathbf{X} = (X_{i,k})$.*

1. *Data are centered around zero with unit variance. i.e $\mathbb{E}[X_{i,k}] = 0$ and $\text{Var}[X_{i,k}] = 1$.*
2. *Data are uniformly bounded. That is, there exists a constant $M > 0$ such that*

$$\mathbb{P}[|X_{i,k}| < M] = 1,$$

3. *The Pearson's correlation estimator is computed by*

$$\widehat{R}_{i,j} = \frac{1}{n} \sum_{c=1}^n X_{i,c} X_{j,c},$$

4. *The population level correlation satisfy*

$$|R_{i,j}| = |\mathbb{E}[X_{i,k} X_{j,k}]| < 1.$$

for all $1 \leq i, j \leq p_n$ and $k = 1, \dots, n$.

Condition 3.2. *There exist constants $c_0 > 0$ and $\tau > 0$, such that*

$$\mu_{\inf} = \inf_{i < j} \{|\mu_{i,j}| : \delta_{i,j}^0 = 1\} = c_0 n^{-1/2+\tau}.$$

Condition 3.3. Let $\tau > 0$ be the same constant in Condition 3.2. Then

$$\log(p_n) = o(n^{2\tau}).$$

Condition 3.4. Suppose there exists $0.5 < \pi_0 < 1$, such that

$$\lim_{n \rightarrow \infty} \pi_0 = \pi_0 \text{ and } \lim_{n \rightarrow \infty} \pi_1 = 1 - \pi_0.$$

Condition 3.5. Given data $\{z_{i,j}\}_{i < j}$, suppose $\hat{f}_c(\cdot)$ be a consistent estimate for $f_c(\cdot)$ for $k = 0, 1$. Suppose $\hat{\pi}_0$ is consistent estimates for π_0 . Specifically, for any $\epsilon > 0$,

$$\lim_{p_n \rightarrow \infty} \mathbb{P}\{\|\hat{f}_c(\cdot) - f_c(\cdot)\|_2 + |\hat{\pi}_0 - \pi_0| > \epsilon\} = 0.$$

where $\|\cdot\|_2$ be the L_2 norm for the function, which is defined as $\|f\|_2 = \int_{\mathbb{R}} \{f(x)\}^2 dx$.

Condition 3.6. Let $\omega = (\sum_{c=1}^C |V_c| \times (|V_c| - 1)/2) / (|V| \times (|V| - 1)/2)$ the proportion of edges inside community networks and $\int_{z_0}^{\infty} f(z_{i,j}) = F(z_0)$. z_0 is the universal threshold cut-off value, $z_{0,in}$ is the within networks threshold cut-off value, $z_{0,out}$ is the within networks threshold cut-off value.

$$\frac{F_0(z_0) - F_0(z_{0,out})}{F_0(z_{0,in}) - F_0(z_0)} > \frac{\omega \pi_0^{in}}{(1 - \omega) \pi_0^{out}}$$

$$\frac{F_1(z_0) - F_1(z_{0,out})}{F_1(z_{0,in}) - F_1(z_0)} < \frac{\omega \pi_1^{in}}{(1 - \omega) \pi_1^{out}}.$$

This condition is generally valid for network induced correlation matrix because by implementing the parsimonious estimation of network topological structure f^{in} is distinct from f^{out} . Thus, we have $\pi_0^{in} \ll \pi_0^{out}$ and $\pi_1^{in} \gg \pi_1^{out}$, and condition holds.

3.2 Tail Probability Bounds

By Berry-Esseen theorem and Taylor expansion, it is straightforward to show the following lemma:

LEMMA 3.1. For any $i < j$,

$$\lim_{n \rightarrow \infty} \sup_{z \in \mathbb{R}} |f_{i,j}(z) - \sqrt{n} \phi\{\sqrt{n}(z - \mu_{i,j})\}| = 0.$$

In addition, we also need to study the probability bound of the $z_{i,j}$. Specifically, we have the following lemma:

LEMMA 3.2. Suppose Condition 3.1 holds. For all $1 \leq i, j \leq p_n$, there exists a constant $K > 0$ and $N > 0$, for and $n > N$, and any $\epsilon > 0$, we have

$$\mathbb{P}[\sqrt{n}|z_{i,j} - \mathbb{E}[z_{i,j}]| > \epsilon] \leq \exp(-K\epsilon^2).$$

By Lemma 3.1 and Condition 3.1, we can uniformly approximate $f_1(z)/f_0(z)$, which is stated in the following lemma:

LEMMA 3.3.

$$\begin{aligned} \lim_{n \rightarrow \infty} \sup_{z \in \mathbb{R}} |f_0(z) - \sqrt{n} \phi\{\sqrt{n}z\}| &= 0, \\ \lim_{n \rightarrow \infty} \sup_{z \in \mathbb{R}} \left| f_1(z) - \frac{1}{q_n} \sum_{i < j} \delta_{i,j}^0 \sqrt{n} \phi\{\sqrt{n}(z - \mu_{i,j})\} \right| &= 0, \end{aligned}$$

and

$$\lim_{n \rightarrow \infty} \sup_{z \in \mathbb{R}} \left| \frac{f_1(z)}{f_0(z)} - \frac{\pi_0}{\pi_1} \frac{\sum_{i < j} \delta_{i,j}^0 \phi\{\sqrt{n}(z - \mu_{i,j})\}}{(p_n(p_n - 1)/2 - q_n) \phi(\sqrt{n}z)} \right| = 0,$$

LEMMA 3.4. Suppose Conditions 3.2–3.4 hold. There exist constants $C_0 > 0$ and $C_1 > 0$ such that for any $i < j$ and any $T > (1 - \pi_0)/\pi_0$, there exists $N_T > 0$, for all $n > N_T$, we have when $e_{i,j} \in G$, then

$$\mathbb{P} \left[\frac{\sum_{i' < j'} \delta_{i',j'}^0 \phi\{\sqrt{n}(z_{i,j} - \mu_{i',j'})\}}{\{p_n(p_n - 1)/2 - q_n\} \phi(\sqrt{n}z_{i,j})} \leq T \right] \leq \exp(-C_1 n^{2\tau}).$$

And when $e_{i,j} \notin G$, then

$$\mathbb{P} \left[\frac{\sum_{i',j'} \delta_{i',j'}^0 \phi\{\sqrt{n}(z_{i,j} - \mu_{i',j'})\}}{\{p_n(p_n - 1)/2 - q_n\} \phi(\sqrt{n}z_{i,j})} > T \right] \leq C_2 \exp(-C_0 n^{2\tau}).$$

Note that N_T depends on T but it does not depend on i and j .

3.3 Selection and Estimation Consistency

We construct the population level selection indicator $\tilde{\delta}_{i,j}(T)$ and the selection indicator estimator $\hat{\delta}_{i,j}(T)$ and discuss their properties in Lemmas 3.5 and 3.6 respectively.

LEMMA 3.5. *Suppose Conditions 3.2–3.4 hold. For all $i < j$ and any $T > (1 - \pi_0)/\pi_0$, let*

$$\tilde{\delta}_{i,j}(T) = I \left[\frac{\pi_1 f_1(z_{i,j})}{\pi_0 f_0(z_{i,j})} > T \right].$$

Then there exist $N_T > 0$, $C_3 > 0$ and $C_4 > 0$ such that for any $n > N_T$,

$$\mathbb{P}\{\tilde{\delta}_{i,j}(T) \neq \delta_{i,j}^0\} \leq C_3 \exp(-C_4 n^{2\tau}).$$

where N_T depends on T but not on i and j , and $\tau > 0$ is the same constant in Condition 3.2.

LEMMA 3.6. *For any $T > (1 - \pi_0)/\pi_0$ and any $i < j$, let*

$$\hat{\delta}_{i,j}(T) = I \left[\frac{\hat{\pi}_1 \hat{f}_1(z_{i,j})}{\hat{\pi}_0 \hat{f}_0(z_{i,j})} > T \right].$$

Then there exists $N_T > 0$ such that for all $n > N_T$,

$$\mathbb{P}[\hat{\delta}_{i,j}(T) \neq \delta_{i,j}^0] \leq C_3 \exp(-C_4 n^{2\tau}),$$

where the constants C_3 , C_4 and τ are the same as the ones in Lemma 3.5.

We establish the selection consistency and estimation consistency in the following two theorems respectively.

THEOREM 1. (*Selection Consistency*) Suppose Conditions 3.1 – 3.5 hold. Denote by $\mathbf{\Delta}_0 = \{\delta_{i,j}^0\}_{i<j}$ all the edge indicators. For any $T > (1 - \pi_0)/\pi_0$, let $\widehat{\mathbf{\Delta}}(T) = \{\widehat{\delta}_{i,j}(T)\}_{i<j}$, then there exists $N_T > 0$ for all $n > N_T$,

$$\mathbb{P}\{\widehat{\mathbf{\Delta}}(T) = \mathbf{\Delta}_0\} \geq 1 - \frac{C_3}{2} p_n (p_n - 1) \exp(-C_4 n^{2\tau}).$$

where the constants C_3 , C_4 and τ are the same as the ones in Lemma 3.5. Furthermore,

$$\lim_{n \rightarrow \infty} \mathbb{P}\{\widehat{\mathbf{\Delta}}(T) = \mathbf{\Delta}_0\} = 1.$$

THEOREM 2. (*Estimation Consistency*) Suppose Conditions 3.1 – 3.5 hold and the constant τ in Condition 3.5 satisfies $0 < \tau < 1/2$. For any $\epsilon > 0$ and any $T > (1 - \pi_0)/\pi_0$, we have

$$\lim_{n \rightarrow \infty} \mathbb{P}[\|\text{NICE}(\widehat{\mathbf{R}}; T) - \mathbf{R}\|_\infty > \epsilon] = 0,$$

where $\|\mathbf{M}\|_\infty$ is the L^∞ norm, i.e. $\|\mathbf{M}\|_\infty = \max_{1 \leq i, j \leq p_n} |m_{i,j}|$ for any matrix $\mathbf{M} = (m_{i,j})$.

3.4 Reduced false positive and negative discovery rates by using NICE thresholding

THEOREM 3. Suppose Condition 3.6 hold, we have both 1) $E(\sum_{i<j} I(\widehat{\delta}_{ij}^{\text{NICE}} = 1 | \delta_{ij} = 0)) \leq E(\sum_{i<j} I(\widehat{\delta}_{ij}^{\text{Univ}} = 1 | \delta_{ij} = 0))$ the expected false positively thresholded edges by using the graph topology oriented thresholding (NICE) method are less than the universal thresholding method; 2) $E(\sum_{i<j} I(\widehat{\delta}_{ij}^{\text{NICE}} = 0 | \delta_{ij} = 1)) \leq E(\sum_{i<j} I(\widehat{\delta}_{ij}^{\text{Univ}} = 0 | \delta_{ij} = 1))$, the expected false negatively thresholded edges by using the graph topology oriented thresholding (NICE) method are less than the universal thresholding method.

4 Data Analysis

4.1 Data examples

We apply the NICE method to two publicly available high-dimensional biomedical data sets. By using these two examples, we show that the latent $G^1 \cup G^0$ mixture structure widely exists in data across platforms (e.g. proteomics, genomics, and imaging data, yet due to space limitation we only demonstrate two data types).

4.1.1 Proteomics data

The first example is matrix-assisted laser desorption ionization time of flight mass spectrometry (MALDI-TOF MS) proteomics data from human 288 subjects (Yildiz *et al*, 2007). The data assess the relative abundance of peptides/proteins in human serum. Each raw mass spectrum consists roughly 70,000 data points. After preprocessing steps including registration, wavelets denoising, alignment, peak detection, quantification, and normalization (Chen *et al*, 2009), 184 features are extracted to represent the most abundant protein and peptide features in the serum. Each feature is located at a distinct m/z value that could be linked to a specific peptide or protein with some ion charges (feature id label). The original paper utilizes the proteomics data to enhance understanding of lung cancer pathology at the molecular level. In this paper, we focus on estimating the correlation matrix to investigate interactive relationships between these features.

We apply NICE to detect correlated peptide/protein networks and estimate correlation matrix based on the Fisher’s Z transformed sample correlation matrix (Figure 2a). First, the penalized objective function 1 is implemented to capture the latent $G^1 \cup G^0$ mixture structure. The estimation results are $\hat{C} = 77$, and that seven significant community networks (G_1) are detected and the rest are singletons (G_0) (see Figure 2b). Figure 2b reorders features Figure 2a by the detected topological structure. Generally, features within networks are more correlated than features outside networks

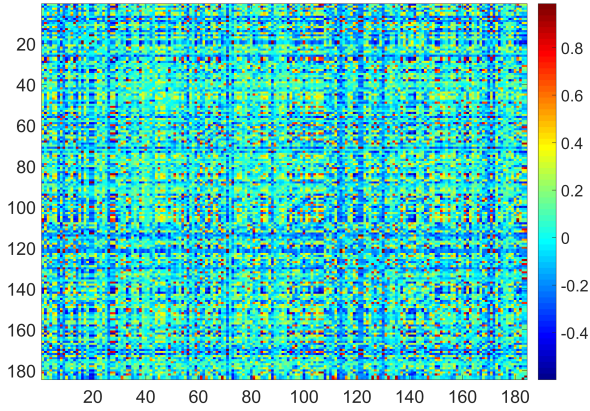
We show that the distributions of edges inside and outside networks in Figure 2c. Clearly, f^{in} and f^{out} show distinct distributions, and f^{out} is close to the null distribution for which all edges are not

connected. We estimate $\hat{\pi}_0^{all} = 0.78$, $\hat{\pi}_0^{out} = 0.83$, and $\hat{\pi}_0^{in} = 0.001$. Then, we apply the network based thresholding to estimate \hat{E} and the correlation matrix. The estimate \hat{E} and thresholding rule $\{\hat{\delta}_{i,j}\}$ are shown in Figure 2d. The network detection results provide informative inferences of the interactive relationship between these proteomics features. In this data example, each network represents a group of related protein and peptides that can be confirmed by proteomics mass spectrometry literature. For example, the most correlated network three consists a list of proteins of normal and variant hemoglobins with one and two charges (Lee *et al*, 2011) including normal hemoglobins α and β with one charge and two charges (at m/z 15127, 15868, 7564, and 7934). The highly correlated networks of biomedical features may provide guidance to identify a set of biomarkers for future research that allow to borrow power between each other.

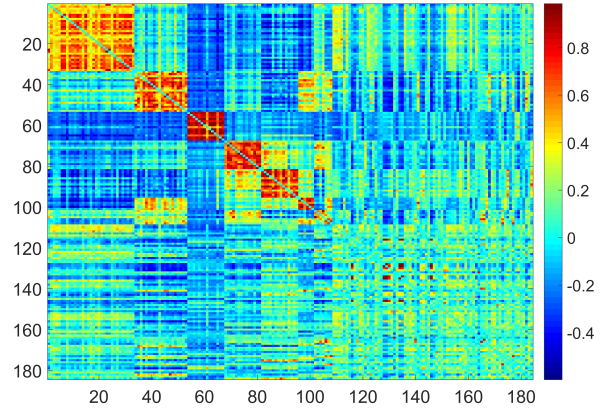
4.1.2 Gene expression data

The second data example is gene expression profiling data based on Affy Human Genome U133A 2.0 array. The data is publicly available at Gene Expression Omnibus (GEO) with accession code: GSE17156, GSE30550, GSE52428 and used by Dream Challenge (see more details at <https://www.synapse.org/#!/Synapse:syn5647810/wiki/399110>). Blood samples were collected for 110 healthy controls at baseline. We focus on 1924 gene expression features that are commonly observed in human blood, and normalized data is used for analysis. The input data for our model is a 1924×1924 sample correlation matrix (Figure 4a). The sample correlation matrix show no explicit organized topological structures. By applying the penalized objective function in 1, we identify the latent $G^1 \cup G^0$ mixture structure (Figure 4b). Note that Figure 4b is a isomorphic graph to Figure 4a with reordered nodes. With $\hat{C} = 613$, four large networks and a long list of singletons and small networks (with 2 or 3 nodes) are detected because of the penalty term.

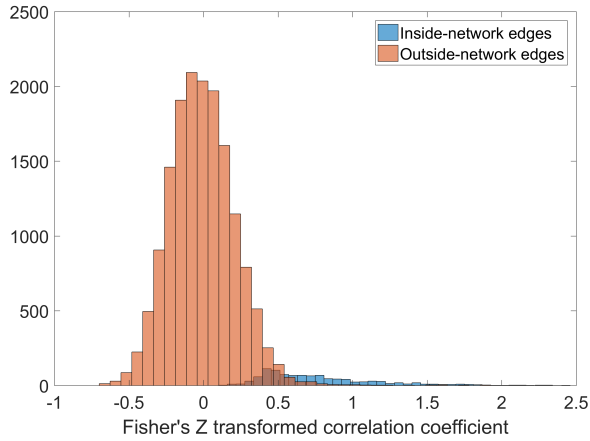
Figure 4c shows that edges inside and outside community networks follow distinct distributions. We estimate $\hat{\pi}_0^{all} = 0.84$, $\hat{\pi}_0^{out} = 0.99$, and $\hat{\pi}_0^{in} = 0.05$. The distribution of edges outside of community networks is also close to the null distribution of non-connected edges, whereas the distribution of edges inside networks again centers around 0.5. By applying the network guided thresholding, we obtain the estimated correlation matrix and \hat{E} as shown in figure 4d.



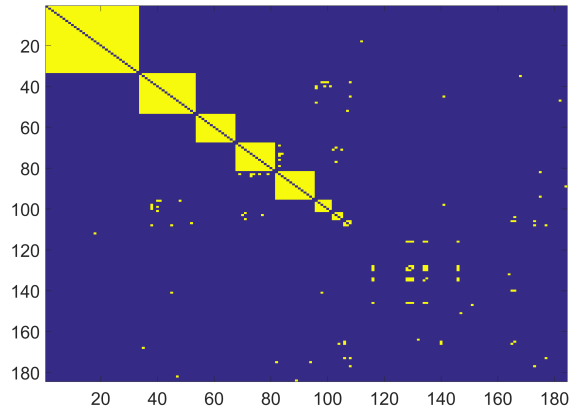
(a) Sample correlation



(b) Detecting latent $G^1 \cup G^0$ mixture structure



(c) Edges inside and outside networks

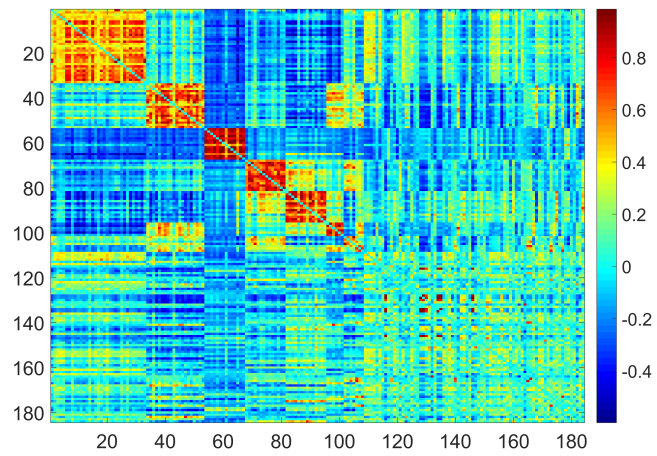


(d) Estimated edge set \hat{E}

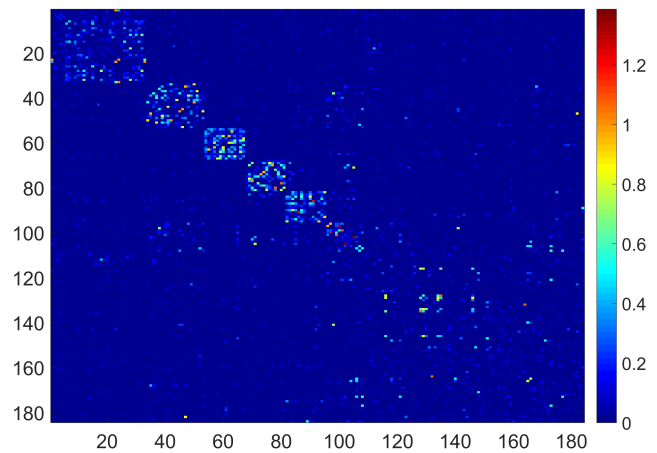
Figure 2: Application of the NICE to the example data set one. (a) is the heatmap of sample correlation matrix; (b) demonstrates the latent $G^1 \cup G^0$ mixture structure by reordering the variables in the heatmap; (c) shows the distributions of edges inside and outside the networks; (d) is the estimated \hat{E} based on the NICE thresholding.

Figure 3: *Glasso* results for Example Data 1: it shows that *Glasso* may false negatively regularize edges to zero in networks (with the sparsity assumption).

(a) Correlation heatmap in the order of detected communities



(b) *glasso* results



Interestingly, the latent $G^1 \cup G^0$ mixture structure shows in both data examples, which can also be identified in large data from many other platforms including neuroimaging activation and connectivity data, DNA methylation data, and etc. (?). In addition, for most of these data sets the inside and outside network edge distributions tend to be distinct with f^{out} close to the null distribution and f^{in} centers around 0.5. This further verifies that our assumptions of mixture distribution and condition ?? are generally valid.

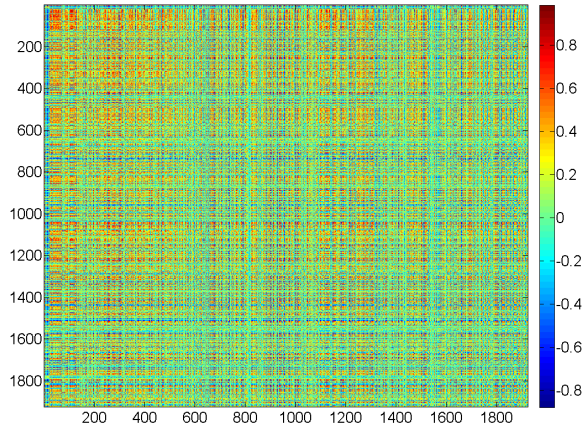
In comparison, when we apply existing methods (e.g. *glasso*), the latent $G^1 \cup G^0$ mixture structure can not be identified based on the estimated covariance or inverse covariance matrix. Many inside network edges are (false negatively) regularized to zero (see Supplementary Materials).

4.2 Simulation Studies

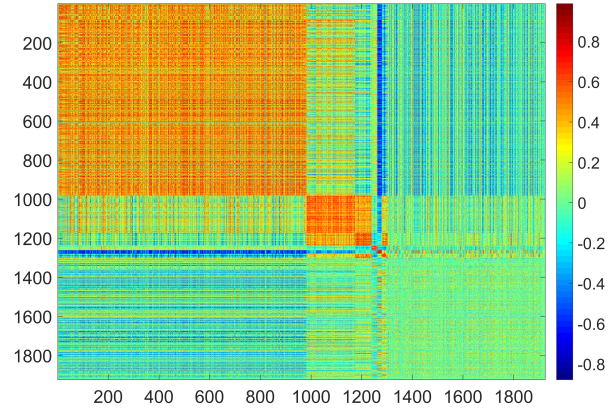
We conduct numerical studies to evaluate the performance of our approach, and compare it with several existing methods.

4.2.1 Synthetic data sets

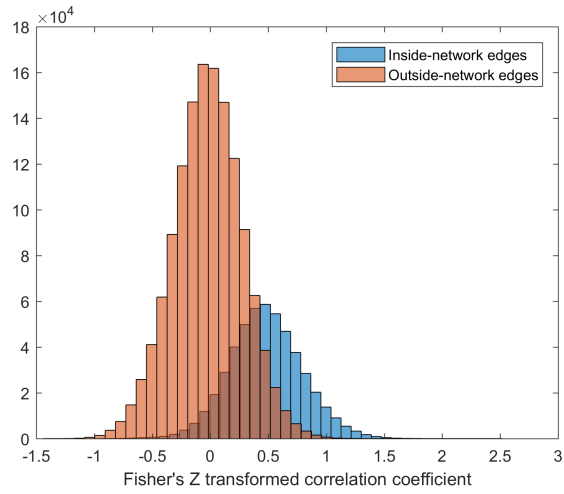
We simulate each data set with $p = 100$ variables, and thus $|V| = 100$ and $|E| = \binom{100}{2} = 4950$. We assume that the correlation matrix includes two community networks, and the first include 15 nodes and the second 10 nodes. The induced networks are complete subgraphs (cliques) that all edges are connected within these two networks and no other edges are connected outside the two networks (Figure 1a). Next, we permute the order of the nodes to mimic the practical data where the topological structure is latent. Figure 1b represents the connected edges in the matrix. Let vector $\mathbf{x}_{p \times 1}^k$ follow a multivariate normal distribution, with zero mean and covariance matrix $\Sigma_{p \times p}$, and the sample size is n . $\sigma_{i,j}$ is an entry at the i th row and j th column of Σ , $\sigma_{i,j} = 1$ if $i = j$ (then $\Sigma = \mathbf{R}$), and $\sigma_{i,j} = \rho$ if $e_{i,j} \in G_c$ (inside network edges) and $\sigma_{i,j} = 0$ when $e_{i,j} \notin G_c$ (outside network edges). We simulate 100 data sets at three different settings with different levels of signal to noise ratio (SNR) by using various sample sizes n and values of ρ . A larger sample size reduces the asymptotic variance of $\hat{\sigma}_{i,j}$ and thus the noise level is lower; and a higher absolute value of ρ



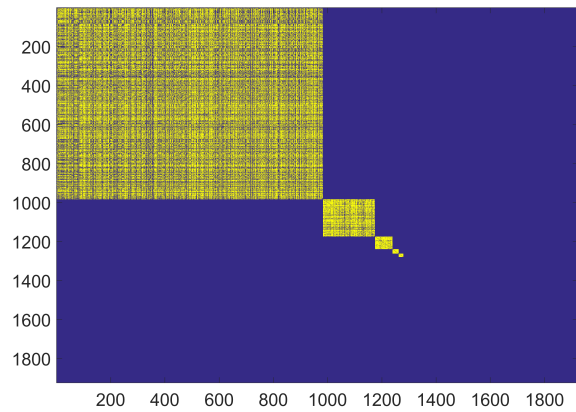
(a) Sample correlation



(b) Weight matrix \mathbf{W}



(c) Edges inside and outside networks



(d) Estimated edge set $\hat{\mathbf{E}}$

Figure 4: Application of the NICE to the example data set two. (a) is the sample correlation matrix; (b) demonstrates the latent $G^1 \cup G^0$ mixture structure by reordering the variables in the heatmap; (c) shows the distributions of edges inside and outside the networks; (d) is the estimated $\hat{\mathbf{E}}$ based on the NICE thresholding.

represents higher signal level. A higher SNR leads to more distinct empirical distributions of $\hat{\sigma}_{i,j}$ between inside network edges $e_{i,j} \in G_c$ and outside network edges $e_{i,j} \notin G_c$. Figure 1c demonstrates a calculated correlation matrix based on a simulated data set.

In our simulated data sets, 150 edges are connected and 4800 edges are unconnected, which together represent the graph edge skeleton E . For both precision matrix shrinkage and covariance matrix thresholding methods we treat a non-zero entry $\hat{\delta}_{i,j} = 1$ (Mazumder and Hastie, 2012) as a connected edge. We summarize the false positive (FP) edges $\hat{\delta}_{i,j} = 1$ when the edge is not connected and $e_{i,j} \notin G_c$ and false negative (FN) edges $\hat{\delta}_{i,j} = 0$ when the edge is connected and $e_{i,j} \in G_c$. We compare FN and FP counts of each method by contrasting the estimated \hat{E} with the truth E . We compare our method with universal thresholding (Thresh), *glasso*, el_1 minimization for inverse matrix estimation (CLIME), and adaptive thresholding (AThres) by comparing the FP and FN edges of estimating the graph edge skeleton E (Bickel and Levina, 08; Friedman *et al*, 2008; Cai *et al*, 2011; Cai and Liu, 2011).

4.2.2 Simulation Study Results

The simulation results are summarized in Table 1. Rather than selecting a single tuning parameter λ for *glasso* and other methods by cross-validation, we explore all possible choices within a reasonable range and use the one with best performance for comparison. Cross the 100 simulation data sets, we summarize the 25%, 50%, and 75% quantiles of the number of FP and FN edges to assess the performance of each method. The results show that the NICE algorithm outperforms the competing methods even when optimal tuning parameters are used (after comparing with the truth) for these methods. One possible reason could be the NICE algorithm thresholds the correlation matrix based on the topological structure rather than the a universal shrinkage or thresholding strategy. More importantly, our approach is the only method can automatically detect the underlying $G^1 \cup G^0$ mixture topological structure. When the graph topological structure does not exist, the performance of all methods are similar across all settings. The matrix norm loss is not compared, because the community networks are small in size and norm comparison are likely determined by the false positive edges outside network communities. We note that the methods with sparsity

Table 1: Median along with 25% and 75% quantiles of FP and FN

Method	Tuning Par.	$\sigma = 0.5, n = 25$				$\sigma = 0.5, n = 50$				$\sigma = 0.7, n = 25$			
		Med.	FP Quantiles	Med.	FN Quantiles	Med.	FP Quantiles	Med.	FN Quantiles	Med.	FP Quantiles	Med.	FN Quantiles
glasso	0.1	1673	(1648, 1702)	59	(55, 64)	1621	(1591.5, 1640)	44	(40, 46)	1581.5	(1557, 1606)	45.5	(42, 48)
	0.2	1008.5	(989, 1025)	59	(53.5, 64.5)	630	(610, 644)	38	(33.5, 43)	932.5	(920, 955.5)	36	(32, 40)
	0.3	546	(529.5, 560)	56	(48, 63.5)	151	(141, 162.5)	38	(30.5, 43)	500.5	(490, 516)	28	(23.5, 33)
	0.4	211.5	(200.5, 222.5)	60	(50.5, 72)	19	(16, 21)	48.5	(38, 58)	194	(186, 204.5)	24.5	(20, 29)
	0.5	51	(46, 59)	80.5	(66, 96)	1	(0, 2)	82.5	(67, 96.5)	47	(41.5, 54)	28	(22.5, 35)
	0.6	7	(5, 10)	112.5	(97, 125.5)	0	(0, 0)	130	(118.5, 137)	6	(5, 8.5)	41	(31, 51)
	0.7	0	(0, 1)	140	(131.5, 146)	0	(0, 0)	149	(147, 150)	0	(0, 1)	75	(61.5, 89)
	0.8	0	(0, 0)	149	(148, 150)	0	(0, 0)	150	(150, 150)	0	(0, 0)	127	(119.5, 135)
	0.9	0	(0, 0)	150	(150, 150)	0	(0, 0)	150	(150, 150)	0	(0, 0)	149	(149, 150)
	1.0	0	(0, 0)	150	(150, 150)	0	(0, 0)	150	(150, 150)	0	(0, 0)	150	(150, 150)
CLIME	0.1	1082.5	(1047.5, 1108)	56	(48, 64.5)	993.5	(981, 1024)	39	(32, 45.5)	1054	(1021, 1079)	48.5	(40, 56)
	0.2	353	(339.5, 367.5)	79.5	(69, 87.5)	241.5	(231.5, 251.5)	61	(54, 67.5)	345	(328, 359)	70	(59, 78)
	0.3	63	(57, 69)	110	(98.5, 115)	25	(22, 29)	92	(84.5, 100)	64	(59, 68)	98	(87, 103)
	0.4	0	(0, 1)	140	(135, 144)	0	(0, 0)	130	(124, 135)	0	(0, 1)	134	(129, 139)
	0.5	0	(0, 0)	150	(150, 150)	0	(0, 0)	150	(150, 150)	0	(0, 0)	150	(150, 150)
Thres	0.1	2017.5	(1963.5, 2067.5)	0	(0, 2)	1978.5	(1944.5, 2021.5)	0	(0, 0)	2021.5	(1968.5, 2061)	0	(0, 1)
	0.3	1292.50	(1252, 1331)	2	(0, 5)	1249.5	(1220.5, 1288.5)	0	(0, 0)	1293.5	(1251, 1341.5)	1	(0, 3)
	0.5	721.5	(699, 752)	5	(1, 12)	689	(673.5, 721)	0	(0, 1)	722	(693, 756)	3	(1, 10.5)
	0.7	344.5	(325, 360)	14	(7, 26.5)	328.5	(311.5, 349.5)	1	(0, 2)	342.5	(324, 363)	10	(3, 21.5)
	0.9	132	(121, 143.5)	30	(18, 45)	129.5	(121, 142)	3	(1, 7)	133	(123.5, 146)	24	(12, 39.5)
	1.1	41.5	(35, 46)	55.5	(40, 78.5)	40.5	(36.5, 47.5)	10	(4.5, 17)	40	(35.5, 46.5)	49.5	(28, 63)
	1.3	9	(6, 10)	92	(74, 112)	10	(8, 12)	25	(13, 37)	9	(6, 11)	78	(54.5, 89)
	1.5	1	(0, 2)	126	(112.5, 137)	2	(1, 3)	50.5	(32.5, 68)	1	(0, 2)	106	(92.5, 114)
	1.7	0	(0, 0)	145	(138.5, 148)	0	(0, 0)	85.5	(67, 102.5)	0	(0, 0)	132.5	(120.5, 138.5)
	1.9	0	(0, 0)	150	(149, 150)	0	(0, 0)	120.5	(105, 130)	0	(0, 0)	147	(144, 149)
AThres	0.3	2593	(2566.5, 2627.5)	2	(0, 5)	2538.5	(2509.5, 2571)	0	(0, 0)	2594	(2563, 2619)	1	(0, 3)
	0.5	1460	(1421.5, 1486)	5	(1, 12)	1412.5	(1379.5, 1440)	0	(0, 1)	1453	(1419.5, 1491)	3	(1, 10.5)
	0.7	691.5	(667, 717)	14	(7, 26.5)	668.5	(646, 697)	1	(0, 2)	695.5	(665.5, 720)	10	(3, 21.5)
	0.9	271.5	(258, 291.5)	30	(18, 45)	265	(252, 283.5)	3	(1, 7)	270.5	(255.5, 288)	24	(12, 39.5)
	1.1	83	(75, 95)	55.5	(40, 78.5)	85	(75.5, 95.5)	10	(4.5, 17)	82	(74, 89.5)	49.5	(28, 63)
	1.3	18	(15, 21)	92	(74, 112)	22	(18.5, 25.5)	25	(13, 37)	18	(14.5, 22)	78	(54.5, 89)
	1.5	2	(1, 4)	126	(112.5, 137)	4	(3, 6)	50.5	(32.5, 68)	3	(1, 3)	106	(92.5, 114)
	1.7	0	(0, 0)	145	(138.5, 148)	0	(0, 1)	85.5	(67, 102.5)	0	(0, 0)	132.5	(120.5, 138.5)
	1.9	0	(0, 1)	150	(149, 150)	0	(0, 0)	120.5	(105, 130)	0	(0, 0)	147	(144, 149)
	NICE	None	44	(15, 98)	3	(0, 27)	11	(1, 30)	0	(0, 4)	32.5	(13.5, 71)	14

assumption (e.g. *lasso* and CLIME) may miss many connected edges (false negative discovery rates are higher) even when small tuning parameter is used (false positive rates are high). Therefore, when a latent topological structure exists the sparsity assumption may not be valid because a cluster of features within a network are all correlated with each other and many of them can be conditionally independent.

In summary, the numerical results demonstrate that our new method not only provides more accurate estimation of the correlation matrix and the edge set E than the competing method, but also automatically detects the community networks where highly correlated edges distribute in an organized fashion.

5 Discussion and Conclusion

We develop a NICE algorithm to bridge the correlation matrix estimation and graph topological structure detection via a flexible empirical Bayesian framework. Recognizing the latent network topological structure not only can reveal underlying biological pathways, but also can guide the decision making procedure of regularization.

The latent $G^1 \cup G^0$ mixture graph structure exist widely in high-throughput biomedical data, however, the conventional network detection and clustering algorithms may not detect it due to the impact of false positive noises. For instance, a few false positive edges may lead to detecting a large networks with low proportion of highly connected edges. The proposed penalized network estimation objective function can identify the mixture structure because it is less affected by false positive noises. Interestingly, we find that the number of networks is related to the penalty term because a larger C generate many singletons. The optimization of the objective function is interestingly linked to the spectral clustering algorithms and the computational speed is affordable.

Next, the new Bayes factor based thresholding approach naturally incorporates detected network topological structure from step one as prior knowledge. The updated thresholding values are determined by each edge’s ‘location’ on the detected graph topological ‘map’. Therefore, edges bor-

row strength with each other with higher precision based on detected topological structure, which also provides a flexible pathway to account for the dependency between edges. With additional information from the detected topological structure and appropriate modeling strategy, our new thresholding approach reduces false positive and false negative rates simultaneously when topological structures exist. Clearly, the performance of graph topological structure detection influences the accuracy of correlation matrix thresholding because it determines the empirical distributions of $z_{i,j}^{in}$ and $z_{i,j}^{out}$ and thus $\hat{\theta}_{in}$ and $\hat{\theta}_{out}$. Therefore, the two steps of the NICE algorithm are seamlessly connected as the parsimonious property of the network detection ensures the efficiency and accuracy of the following regularization step. Edges outside networks are subject to more stringent thresholds whereas edges inside networks are less likely to be thresholded. This decision rule is data-oriented and determined by the latent spatial distributions of edges in the sample correlation matrix. Last but not least, we develop theoretical results to prove the consistency of edge selection and estimation.

In our application, only positive (correlation) edges are distributed in an organized graph topology and the negative (correlation) edges are randomly distributed. Based on the network based thresholding, negative (correlation) edges are thresholded. Our methods are ready to be extended to the scenario that negatively correlated edges show a organized topological structure. The numerical studies and example data application have demonstrated excellent performance of the NICE algorithm regarding false positive/negative findings and latent network detection. The computational cost of NICE algorithm is low (for our simulation example the algorithm only takes 40 seconds using i7 CPU and 24G memory), and thus it is ready to scale up for larger data sets. In addition, the NICE algorithm is not restricted for multivariate Gaussian distributed data and it is straightforward to extend the sample correlation matrix to other sample metrics, for example maximal information coefficients (Kinney and Atwal, 2014) for continuous data and polychoric correlation coefficient for categorical data (Bonett and Price, 2005) because graph topology oriented thresholding are based on the empirical distribution of the coefficients.

Acknowledgements

The research is based upon work supported by the Office of the Director of National Intelligence (ODNI), Intelligence Advanced Research Projects Activity (IARPA), via DJF-15-1200-K-0001725.

A Appendix

A.1 A new algorithm to optimize the objective function 1

The objective function

$$\arg \max_{C, \{G_c\}} \sum_{C=1}^C \exp\{\log(\sum (w_{i,j}|e_{i,j} \in G_c)) - \lambda_0 \log(|E_c|)\}$$

is non-convex and NP hard. We solve it in two steps.

λ_0 is between 0 and 1, by default we set $\lambda_0 = 1/2$ because we aim to include most informative edges in . Firstly, we optimize $\{G_c\}$ with given C :

$$\begin{aligned} & \arg \max_{\{G_c\}} \sum_{C=1}^C \exp\{\log(\sum (w_{i,j}|e_{i,j} \in G_c)) - \lambda_0 \log(|E_c|)\} \\ = & \arg \max_{\{G_c\}} \sum_{C=1}^C \left(\frac{\sum (w_{i,j}|e_{i,j} \in G_c)}{|E_c|} \right)^{\lambda_0} \left(\sum (w_{i,j}|e_{i,j} \in G_c) \right)^{1-\lambda_0} \\ \doteq & \arg \max_{\{G_c\}} \sum_{C=1}^C \rho_{CC} |V_c|, \text{ when } \lambda_0 = 1/2, \rho_{CC} = \sum (w_{i,j}|e_{i,j} \in G_c) / |E_c| \\ = & \arg \max_{\{G_c\}} \sum (w_{i,j}|e_{i,j} \in G) / |V| - \sum_{C=1}^C \sum_{C' \neq C} \rho_{CC'} (|V_c| + |V_{C'}|) \tag{3} \\ \Leftrightarrow & \arg \min_{\{G_c\}} \sum_{C=1}^C \sum_{C' \neq C} \rho_{CC'} (|V_c| + |V_{C'}|) \\ = & \arg \min_{\{G_c\}} \sum_{C=1}^C \sum_{C' \neq C} \frac{\sum (w_{i,j}|i \in G_c, j \in G_{C'})}{|V_c| |V_{C'}|} (|V_c| + |V_{C'}|) \\ = & \arg \min_{\{G_c\}} \sum_{C=1}^C \frac{\sum (w_{i,j}|i \in G_c, j \notin G_C)}{|V_c|} \end{aligned}$$

We solve objective function 3 by using spectral clustering algorithm RatioCut (Chen *et al*, 2015a).

Next, we select C by grid searching that maximizes the criteria:

$$\sum_{C=1}^C \left(\frac{\sum(w_{i,j}|e_{i,j} \in G_c)}{|E_c|} \right)^{\lambda_0} \left(\sum(w_{i,j}|e_{i,j} \in G_c) \right)^{1-\lambda_0}$$

At this step, a larger λ_0 often leads to detected subnetworks with higher proportion of more informative edges and smaller sizes whereas a smaller λ_0 often produces larger networks including more informative edges in G . The iterations of the above two steps implement the optimization of 1.

When a more complex subgraph topological structure of G_c (e.g. bipartite subgraph) exists in G instead of the default clique structure, advanced graph topology detection tools are needed (e.g. Chen *et al*, 2016). The detected organized subnetworks (with more complex graph topological structures) can increase the objective function 1 as the quality term increases and quantity term is almost unchanged. Therefore, the refined graph topological structure detection algorithms, for instance, K-partite, rich-club, and overlapped subgraphs could further assist to optimize the objective function. In future, more graph topological structure automatic detection tools will be developed, which will be compatible with the objective function 1.

A.2 W matrix calculation

Let $z_{i,j}$ be the Fisher's Z transformed correlation coefficient $\widehat{R}_{i,j}$, for instance (Kendall's Tau or other pairwise relationship metrics could also be applied). We could simply let $w_{i,j} = z_{i,j}$ or further transform it to the probability scale. Assume that sample correlation coefficients for all edges follow a mixture distribution $z_{i,j} \sim \pi_0 f_0(z_{i,j}) + \pi_1 f_1(z_{i,j})$ where $\pi_0 + \pi_1 = 1$ (Efron, 2004; Wu *et al*, 2006; Efron, 2007). f_1 represents the distribution of correlations corresponding to the component of connected edges $z_{i,j} | (\delta_{i,j} = 0) \sim f_0(z_{i,j})$, and f_0 for the unconnected edges $z_{i,j} | (\delta_{i,j} = 1) \sim f_1(z_{i,j})$. We adopt the empirical Bayes method to obtain $\hat{\pi}_0, \hat{\pi}_1, \hat{f}_0, \hat{f}_1$, (Efron, 2007) and then $w_{i,j}$ is the posterior probability that $z_{i,j}$ from the non-null component.

A.3 Convenient thresholding value calculation

We calculate the thresholding values for edges inside-networks or outside-networks separately, and these cut-offs can be linked to the overall local fdr value. Therefore, the computation is more straightforward by using the following cut-offs.

An edge inside networks z^{in} is truly connected if $fdr^{in}(z^{in}) \leq 1/(T + 1)$, where T is the threshold. Equivalently if $\frac{f_1(z)}{f_0(z)} \geq T \frac{\pi_0^{in}}{\pi_1^{in}}$, we consider the edge is connected by using the fact below.

$$\begin{aligned} \frac{\pi_1^{in} f_1(z^{in})}{\pi_0^{in} f_0(z)} &= (1 - fdr^{in}(z^{in}))/fdr^{in}(z^{in}) \geq T \\ \Rightarrow \frac{f_1(z^{in})}{f_0(z^{in})} &\geq T \frac{\pi_0^{in}}{\pi_1^{in}} \end{aligned} \quad (4)$$

The above cut-off can be linked to $fdr^{all}(z^{in})$ by using the fact that

$$\begin{aligned} \frac{f_1(z^{in})}{f_0(z^{in})} &\geq T \frac{\pi_0^{in}}{\pi_1^{in}} \\ \Rightarrow \frac{f_1(z^{in})}{f_0(z^{in})} \frac{\pi_1^{all}}{\pi_0^{all}} &= (1 - fdr^{all}(z^{in}))/fdr^{all}(z^{in}) \geq T \frac{\pi_0^{in}}{\pi_1^{in}} \frac{\pi_1^{all}}{\pi_0^{all}} \\ \Rightarrow fdr^{all}(z^{in}) &= \frac{1}{T \frac{\pi_0^{in}}{\pi_1^{in}} \frac{\pi_1^{all}}{\pi_0^{all}} + 1} \end{aligned} \quad (5)$$

For example, if $T = 4$, $\pi_0^{in}/\pi_1^{in} = 0.1$ and $\pi_1^{all}/\pi_0^{all} = 0.1$, then $fdr^{all}(z^{in})=0.96$ and most edges inside networks are considered as connected because the topological structure suggests that threshold is loose.

Similarly, for edges outside networks

$$fdr^{all}(z^{out}) = \frac{1}{T \frac{\pi_0^{out}}{\pi_1^{out}} \frac{\pi_1^{all}}{\pi_0^{all}} + 1}$$

if $T = 4$, $\pi_0^{out}/\pi_1^{out} = 40$ and $\pi_1^{all}/\pi_0^{all} = 0.1$, then $fdr^{all}(out)=0.06$ and most edges outside the network are thresholded by using a more stringent cut-off.

By using these overall fdr based thresholds, the computation is faster. More importantly, we can

note how topological structure and edge distributions can jointly impact the decision making process of the correlation matrix thresholding. When the data shows no network structure, for instance, $\pi_0^{in}/\pi_1^{in} = \pi_0^{out}/\pi_1^{out} = 10$ and $\pi_1^{all}/\pi_0^{all} = 10$, then $fdr^{all}(in) = fdr^{all}(out) = 0.2$. Our thresholding rule boils down to the universal thresholding rule.

A.4 NICE algorithm

The following is the detailed NICE algorithm.

Algorithm 1 NICE algorithm

- 1: **procedure** NICE-ALGORITHM
 - 2: Obtain the empirical Bayes fuzzy logic matrix $\mathbf{W} = g(\widehat{\mathbf{R}})$;
 - 3: Calculate the Laplacian matrix $\mathbf{L} = \mathbf{D} - \mathbf{W}$
 - 4: **for** cluster number $C = 2 : |V| - 1$ **do**
 - 5: Compute the first C eigenvectors $[u_2, \dots, u_C]$ of L , with eigenvalues ranked from the smallest;
 - 6: Let $U = [u_2^T, \dots, u_C^T]$ be a $|V| \times C$ matrix containing all $C - 1$ eigenvectors;
 - 7: Perform K-means clustering algorithm on U with number of clusters of C to cluster $|V|$ nodes into C networks;
 - 8: Calculate the ‘quality and quantity’ criterion for each C .
 - 9: **end for**
 - 10: Adopt the clustering results using the C of the maximum score of the ‘quality and quantity’ criterion.
 - 11: Identify the networks with significantly high proportion of correlated edges by using permutation test: for each detected community network G_c in G
 - i) calculate the $T_c^0 = -\log(1 - \frac{1}{\Gamma(|E_c|)}\gamma(|E_c|, \sum_{i,j \in G_c} -\log(W_{i,j})))$, where Γ is the upper incomplete gamma function and γ is the lower incomplete gamma function;
 - ii) list all $\{W_{i,j}\}$ in \mathbf{W} as a vector and shuffle the order of the vector and assemble the shuffled vector as a permuted \mathbf{W}^m for M (e.g. 10,000) times;
 - iii) calculate the maximum statistic T_{max}^m for all detected communities in each iteration;
 - iv) calculate the percentile of T_c^0 in $\{T_{max}^m\}$, if it is less than the α level then the network G_c is considered as a true community network.
 - 12: Implement the topological structure oriented thresholding strategies for covariance entries inside and outside networks (see details in 2.2)
 - 13: **end procedure**
-

A.5 Proof of Lemma 3.2

Proof. For any i, j , let $Y_c = X_{i,k}X_{j,k}$. Then Y_1, \dots, Y_n are independent and identically distributed.

By Condition 3.1, $P[|Y_c| < M^2] = 1$. Define

$$z_{i,j} = g(Y_1, \dots, Y_l, \dots, Y_n) = \frac{1}{2} \log \left(\frac{1 + \sum_{c \neq l}^n Y_c/n + Y_l/n}{1 - \sum_{c \neq l}^n Y_c/n - Y_l/n} \right).$$

Then for all $l = 1, \dots, n$, by Taylor expansion, we have

$$\begin{aligned} & g(Y_1, \dots, Y_l, \dots, Y_n) - g(Y_1, \dots, Y'_l, \dots, Y_n) \\ &= \sum_{c=1}^{\infty} \frac{\partial^c g}{\partial Y_l^c}(Y_1, \dots, Y'_l, \dots, Y_n) \frac{(Y_l - Y'_l)^c}{k!} \end{aligned}$$

where

$$\frac{\partial^c g}{\partial Y_l^c}(Y_1, \dots, Y'_l, \dots, Y_n) = \frac{(k-1)!}{2n^c} \left(\frac{(-1)^{k+1}}{(1 + \widehat{R}_{i,j})^c} + \frac{1}{(1 - \widehat{R}_{i,j})^c} \right),$$

By Condition 3.1, $|R_{i,j}| < 1$ and strong law of large number, $\widehat{R}_{i,j} < 1$ with probability one. Thus, there exists $N > 0$ and $K_0 > 0$, for all $n > N$, we have

$$\sup_{Y_1, \dots, Y_n, Y'_l} |g(Y_1, \dots, Y_l, \dots, Y_n) - g(Y_1, \dots, Y'_l, \dots, Y_n)| \leq \frac{K_0}{n}$$

By the McDiarmid inequality, for all $n \geq N$, we have

$$P[|z_{i,j} - \mathbb{E}[z_{i,j}]| > \epsilon] \leq \exp \left(-\frac{2n\epsilon^2}{K_0^2} \right).$$

Thus,

$$P[\sqrt{n}|z_{i,j} - \mathbb{E}[z_{i,j}]| > \epsilon] \leq \exp \left(-\frac{2}{K_0^2} \epsilon^2 \right).$$

Taking $K = 2/K_0^2 > 0$ completes the proof. □

A.6 Proof of Lemma 3.4

Proof. When $e_{i,j} \in G$ and $\mu_{i,j} > 0$, then

$$\begin{aligned}
& \mathbb{P} \left[\frac{\sum_{i',j'} \delta_{i',j'}^0 \phi\{\sqrt{n}(z_{i,j} - \mu_{i',j'})\}}{\{p_n(p_n - 1)/2 - q_n\} \phi(\sqrt{n}z_{i,j})} \leq T \right] \\
& \leq \mathbb{P} \left[\frac{\phi\{\sqrt{n}(z_{i,j} - \mu_{i,j})\}}{\{p_n(p_n - 1)/2 - q_n\} \phi(\sqrt{n}z_{i,j})} \leq T \right] \\
& = \mathbb{P} \left[-(z_{i,j} - \mu_{i,j})^2 + z_{i,j}^{2(n)} \leq \frac{2}{n} [\log(T) + \log\{p_n(p_n - 1)/2 - q_n\}] \right] \\
& = \mathbb{P} \left[z_{i,j} \leq \frac{1}{2} \mu_{i,j} + \frac{1}{\mu_{i,j} n} [\log(T) + \log\{p_n(p_n - 1)/2 - q_n\}] \right] \\
& = \mathbb{P} \left[\sqrt{n}(z_{i,j} - \mu_{i,j}) \leq -\sqrt{n}\mu_{i,j}/2 + \frac{1}{\mu_{i,j}\sqrt{n}} \{\log(T) + \log\{p_n(p_n - 1)/2 - q_n\}\} \right] \\
& \leq \mathbb{P} \left[\sqrt{n}(z_{i,j} - \mu_{i,j}) \leq -\sqrt{n}\mu_{\inf}/2 + \frac{1}{\mu_{\sup}\sqrt{n}} \{\log(T) + \log(\{p_n(p_n - 1)/2 - q_n\})\} \right],
\end{aligned}$$

where $\mu_{\sup} = \sup_{i,j} \{|\mu_{i,j}| : e_{i,j} \in G\}$ and μ_{\inf} is defined in Condition 3.2. Note that $\mathbb{E}[z_{i,j}] = \mu_{i,j} + o(n^{-1/2})$. There exists N_2 , for all $n > N_2$, such that $\sqrt{n}(\mu_{i,j} - \mathbb{E}[z_{i,j}]) < 1$. Then $-\sqrt{n}\mathbb{E}[z_{i,j}] - 1 < -\sqrt{n}\mu_{i,j}$ and thus,

$$\begin{aligned}
& \mathbb{P} \left[\sqrt{n}(z_{i,j} - \mu_{i,j}) \leq -\sqrt{n}\mu_{\inf}/2 + \frac{1}{\mu_{\sup}\sqrt{n}} \{\log(T) + \log(p_n(p_n - 1)/2 - q_n)\} \right] \\
& \leq \mathbb{P} \left[\sqrt{n}(z_{i,j} - \mathbb{E}[z_{i,j}]) \leq -\sqrt{n}\mu_{\inf}/2 + \frac{1}{\mu_{\sup}\sqrt{n}} \{\log(T) + \log(p_n(p_n - 1)/2 - q_n)\} + 1 \right]
\end{aligned}$$

By Condition 3.2, we have $\mu_{\inf} = c_0 n^{-1/2+\tau}$ with $\tau > 0$, then $\mu_{\sup} > c_0 n^{-1/2+\tau}$. Also, by Conditions 3.3 and 3.4, we have $\log\{p_n(p_n - 1)/2 - q_n\} = o(n^{2\tau})$, then there exists N_1 such that for all $n > N_1$ we have $n^{-\tau} \log\{T(p_n(p_n - 1)/2 - q_n)\} < c_0^2 n^\tau / 8$ and $n^\tau > 8/c_0$. By Lemma 3.2,

$$\begin{aligned}
& \mathbb{P} \left[\frac{\sum_{i',j'} \delta_{i',j'}^0 \phi\{\sqrt{n}(z_{i,j} - \mu_{i',j'})\}}{\{p_n(p_n - 1)/2 - q_n\} \phi(\sqrt{n}z_{i,j})} \leq T \right] \\
& \leq \mathbb{P} \left[\sqrt{n}(z_{i,j} - \mu_{i,j}) \leq -\frac{c_0}{4} n^\tau \right] \leq \exp \left(-\frac{c_0^2 K n^{2\tau}}{16} \right).
\end{aligned}$$

When $\mu_{i,j} < 0$, based on similar arguments, we have

$$\begin{aligned} & \mathbb{P} \left[\frac{\sum_{i',j'} \delta_{i',j'}^0 \phi\{\sqrt{n}(z_{i,j} - \mu_{i',j'})\}}{\{p_n(p_n - 1)/2 - q_n\} \phi(\sqrt{n}z_{i,j})} \leq T \right] \\ & \leq \mathbb{P} \left[-\sqrt{n}(z_{i,j} - \mu_{i,j}) \leq -\frac{c_0}{4}n^\tau \right] \leq \exp\left(-\frac{c_0^2 K n^{2\tau}}{16}\right). \end{aligned}$$

Taking $C_1 = c_0^2 K/16$ completes the proof for the case when $e_{i,j} \in G$.

When $e_{i,j} \notin G$, then

$$\begin{aligned} & \mathbb{P} \left[\frac{\sum_{i',j'} \delta_{i',j'}^0 \phi\{\sqrt{n}(z_{i,j} - \mu_{i',j'})\}}{(p_n(p_n - 1)/2 - q_n) \phi(\sqrt{n}z_{i,j})} > T \right] \\ & \leq \mathbb{P} \left[\frac{q_n \phi\{\sqrt{n}(z_{i,j} - \mu_{\inf}/3)\}}{(p_n(p_n - 1)/2 - q_n) \phi(\sqrt{n}z_{i,j})} > T, |z_{i,j}| \leq \mu_{\inf}/3 \right] \\ & \quad + \mathbb{P} \left[\frac{\sum_{i',j'} \delta_{i',j'}^0 \phi\{\sqrt{n}(z_{i,j} - \mu_{i',j'})\}}{(p_n(p_n - 1)/2 - q_n) \phi(\sqrt{n}z_{i,j})} > T, |z_{i,j}| > \mu_{\inf}/3 \right] \\ & \leq \mathbb{P} \left[\sqrt{n}z_{i,j} > \sqrt{n}(\mu_{\inf}/6) + \frac{3}{\mu_{\inf}\sqrt{n}} \log \left(T \times \frac{p_n(p_n - 1)/2 - q_n}{q_n} \right) - 1 \right] + \mathbb{P} [|z_{i,j}| > \mu_{\inf}/3]. \end{aligned}$$

By Condition 3.4, $\lim_{n \rightarrow \infty} \log\{(p_n(p_n - 1)/2 - q_n)/q_n\} = \pi_0/(1 - \pi_0)$, there exists N_0 such that for all $n > N_0$, $\log\{T(p_n(p_n - 1)/2 - q_n)/q_n\} > 0$ and $n^\tau > 12/c_0$. Thus,

$$\begin{aligned} & \mathbb{P} \left[\frac{\sum_{i',j'} \delta_{i',j'}^0 \phi\{\sqrt{n}(z_{i,j} - \mu_{i',j'})\}}{(p_n(p_n - 1)/2 - q_n) \phi(\sqrt{n}z_{i,j})} > T \right] \\ & \leq \mathbb{P} [\sqrt{n}z_{i,j} > c_0 n^\tau/12] + \mathbb{P} [\sqrt{n}|z_{i,j}| > c_0 n^\tau/3] \leq 3 \exp\left(-\frac{c_0^2 K}{144} n^{2\tau}\right). \end{aligned}$$

Taking $C_0 = c_0^2 K/144$, $C_2 = 3$ and $N_T = \max\{N_0, N_1, N_2\}$ completes the proof for all the cases. \square

A.7 Proof Lemma 3.5

Proof. Since $T > (1 - \pi_0)/\pi_0$. Then there exists $\epsilon > 0$ such that $T - \epsilon > (1 - \pi_0)/\pi_0$. By Lemma 3.3 and Condition 3.4, there exists $N_1 > 0$, for all $n > N_1$ such that

$$\frac{\pi_1 f_1(z_{i,j})}{\pi_0 f_0(z_{i,j})} > \frac{\sum_{i',j'} \delta_{i',j'}^0 \phi\{\sqrt{n}(z_{i,j} - \mu_{i',j'})\}}{(p_n(p_n - 1)/2 - q_n) \phi(\sqrt{n}z_{i,j})} - \epsilon,$$

$$\frac{\pi_1 f_1(z_{i,j})}{\pi_0 f_0(z_{i,j})} < \frac{\sum_{i',j'} \delta_{i',j'}^0 \phi\{\sqrt{n}(z_{i,j} - \mu_{i',j'})\}}{(p_n(p_n - 1)/2 - q_n) \phi(\sqrt{n}z_{i,j})} + \epsilon.$$

Then by Lemma 3.4, when $e_{i,j} \in G$, then $\delta_{i,j}^0 = 1$ and

$$\begin{aligned} \mathbb{P}[\tilde{\delta}_{i,j}(T) = 0] &= \mathbb{P}\left[\frac{\pi_1 f_1(z_{i,j})}{\pi_0 f_0(z_{i,j})} \leq T\right] \\ &\leq \mathbb{P}\left[\frac{\sum_{i',j'} \delta_{i',j'}^0 \phi\{\sqrt{n}(z_{i,j} - \mu_{i',j'})\}}{(p_n(p_n - 1)/2 - q_n) \phi(\sqrt{n}z_{i,j})} \leq T + \epsilon\right] \leq \exp(-C_1 n^{2\tau}). \end{aligned}$$

when $e_{i,j} \notin G$, then $\delta_{i,j}^0 = 0$ and

$$\begin{aligned} \mathbb{P}[\tilde{\delta}_{i,j}(T) = 1] &= \mathbb{P}\left[\frac{\pi_1 f_1(z_{i,j})}{\pi_0 f_0(z_{i,j})} > T\right] \\ &\leq \mathbb{P}\left[\frac{\sum_{i',j'} \delta_{i',j'}^0 \phi\{\sqrt{n}(z_{i,j} - \mu_{i',j'})\}}{(p_n(p_n - 1)/2 - q_n) \phi(\sqrt{n}z_{i,j})} > T - \epsilon\right] \leq C_2 \exp(-C_0 n^{2\tau}). \end{aligned}$$

Taking $C_3 = \max\{1, C_2\}$ and $C_4 = \min\{C_0, C_1\}$, thus,

$$\Pr[\tilde{\delta}_{i,j}(T) \neq \delta_{i,j}^0] \leq C_3 \exp(-C_4 n^{2\tau}).$$

□

Proof of Lemma 3.6

Proof. Since $T > (1 - \pi_0)/\pi_0$, then there exists $\epsilon > 0$ such that $T - \epsilon > (1 - \pi_0)/\pi_0$. By Condition 3.5, there exists $N_0 > 0$, for all $n > N_0$ and all i, j such that

$$\frac{\widehat{\pi}_1 \widehat{f}_1(z_{i,j})}{\widehat{\pi}_0 \widehat{f}_0(z_{i,j})} > \frac{\pi_1 f_1(z_{i,j})}{\pi_0 f_0(z_{i,j})} - \epsilon, \quad \text{and} \quad \frac{\widehat{\pi}_1 \widehat{f}_1(z_{i,j})}{\widehat{\pi}_0 \widehat{f}_0(z_{i,j})} < \frac{\pi_1 f_1(z_{i,j})}{\pi_0 f_0(z_{i,j})} + \epsilon.$$

By Lemma 3.6, When $e_{i,j} \in G$, then $\mathbb{P}[\widehat{\delta}_{i,j}(T) = 0] \leq \mathbb{P}[\tilde{\delta}_{i,j}(T + \epsilon) = 0] \leq C_3 \exp(-C_4 n^{2\tau})$, and when $e_{i,j} \notin G$, then $\mathbb{P}[\widehat{\delta}_{i,j}(T) = 1] \leq \mathbb{P}[\tilde{\delta}_{i,j}(T - \epsilon) = 1] \leq C_3 \exp(-C_4 n^{2\tau})$. □

A.8 Proof of Theorem 1

Proof. By Lemma 3.6 and the Bonferroni inequality,

$$\begin{aligned} \mathbb{P}\{\widehat{\Delta}(T) \neq \Delta_0\} &= \mathbb{P}\left[\bigcup_{i < j} \{\widehat{\delta}_{i,j}(T) \neq \delta_{i,j}^0\}\right] \\ &\leq \sum_{1 \leq i < j \leq p_n} \mathbb{P}\left[\widetilde{\delta}_{i,j}(T) \neq \delta_{i,j}^0\right] \leq \frac{C_3}{2} p_n(p_n - 1) \exp(-C_4 n^{2\tau}). \end{aligned}$$

By Condition 3.3, $\lim_{n \rightarrow \infty} p_n(p_n - 1) \exp(-C_4 n^{2\tau}) = 0$. This completes the proof. \square

A.9 Proof of Theorem 2

Proof. Note that

$$\begin{aligned} &\mathbb{P}[\|\text{NICE}(\widehat{\mathbf{R}}; T) - \mathbf{R}\|_\infty > \epsilon] \\ &= \mathbb{P}[\|\text{NICE}(\widehat{\mathbf{R}}; T) - \mathbf{R}\|_\infty > \epsilon; \widehat{\Delta}(T) = \Delta_0] + \mathbb{P}[\|\text{NICE}(\widehat{\mathbf{R}}; T) - \mathbf{R}\|_\infty > \epsilon; \widehat{\Delta}(T) \neq \Delta_0] \\ &\leq \mathbb{P}\left[\max_{i < j, e_{i,j} \in G} |\widehat{R}_{i,j} - R_{i,j}| > \epsilon\right] + \mathbb{P}[\widehat{\Delta}(T) \neq \Delta_0] \end{aligned}$$

By Bonferroni inequality and Hoeffding's inequality, we have

$$\mathbb{P}\left[\max_{i < j, e_{i,j} \in G} |\widehat{R}_{i,j} - R_{i,j}| > \epsilon\right] \leq \sum_{i < j, e_{i,j} \in G} \mathbb{P}[|\widehat{R}_{i,j} - R_{i,j}| > \epsilon] \leq q_n \exp\left(-\frac{n\epsilon^2}{2M^4}\right).$$

By Conditions 3.3 and 3.4, $q_n = o(n^{2\tau})$. Since $0 < \tau < 1/2$, then $\lim_{n \rightarrow \infty} q_n \exp(-n\epsilon^2/2M^4) = 0$.

By Theorem 1, we have $\lim_{n \rightarrow \infty} \mathbb{P}[\widehat{\Delta}(T) \neq \Delta_0] = 0$. This completes the proof. \square

A.10 Proof of Theorem 3

Proof. Applying the universal decision rule with z_0 as threshold:

$$E(\#FP) = m \int_{z_0}^{\infty} \frac{\pi_0 f_0(z)}{f(z)} f(z) dz = m\pi_0 F_0(z_0) = m\omega\pi_0^{in} F_0(z_0) + m(1-\omega)\pi_0^{out} F_0(z_0) \quad (6)$$

where $\int_{z_0}^{\infty} f = F(z_0)$ and m is the total number of edges $m = |E|$.

For edges in communities:

$$E^{in}(\#FP) = \omega m \int_{z_{in}}^{\infty} \frac{\pi_0^{in} f_0^{in}(z)}{f^{in}(z)} f^{in}(z) dz = \omega m \pi_0^{in} F_0^{in}(z_{in}) \quad (7)$$

For edges outside communities:

$$E^{out}(\#FP) = (1-\omega)m \int_{z_{0,out}}^{\infty} \frac{\pi_0^{out} f_0^{out}(z)}{f^{out}(z)} f^{out}(z) dz = (1-\omega)m\pi_0^{out} F_0^{out}(z_{0,out}) \quad (8)$$

where $z_{0,in} < z_0 < z_{0,out}$, and $F_0^{out}(z) = F_0^{in}(z) = F_0(z)$. There we expect $E(\#FP) (6) > E^{in}(\#FP) + E^{out}(\#FP) (7 + 8)$ if

$$\begin{aligned} & -\omega m \pi_0^{in} (F_0(z_{in}) - F_0(z_0)) + (1-\omega)m\pi_0^{out} (F_0(z_0) - F_0(z_{0,out})) > 0, \\ \Leftrightarrow & \frac{F_0(z_0) - F_0(z_{0,out})}{F_0(z_{0,in}) - F_0(z_0)} > \frac{\omega\pi_0^{in}}{(1-\omega)\pi_0^{out}} \end{aligned} \quad (9)$$

We further calculate the expected number of true positive (TP) edges using universal threshold and in/out communities to evaluate the power of our network based thresholding.

Applying the universal decision rule with z_0 as threshold:

$$E(\#TP) = m \int_{z_0}^{\infty} \frac{\pi_1 f_1(z)}{f(z)} f(z) dz = m\pi_1 F_0(z_0) = m\omega\pi_1^{in} F_1(z_0) + m(1-\omega)\pi_1^{out} F_1(z_0) \quad (10)$$

For edges in communities:

$$E^{in}(\# TP) = \omega m \int_{z_{in}}^{\infty} \frac{\pi_1^{in} f_1^{in}(z)}{f^{in}(z)} f^{in}(z) dz = \omega m \pi_1^{in} F_1^{in}(z_{in}) \quad (11)$$

For edges outside communities:

$$E^{out}(\# TP) = (1 - \omega) m \int_{z_{out}}^{\infty} \frac{\pi_1^{out} f_1^{out}(z)}{f^{out}(z)} f^{out}(z) dz = (1 - \omega) m \pi_1^{out} F_1^{out}(z_{out}) \quad (12)$$

where $z_{0,in} < z_1 < z_{0,out}$, and $F_1^{out}(z) = F_1^{in}(z) = F_1(z)$. There we expect $E(\#TP)$ (10) $<$ $E^{in}(\#TP) + E^{out}(\#TP)$ (11 + 12) (i.e. $E(\#FN) > E^{in}(\#FN) + E^{out}(\#FN)$) if

$$\begin{aligned} & -\omega m \pi_0^{in} (F_1(z_{in}) - F_1(z_0)) + (1 - \omega) m \pi_1^{out} (F_1(z_0) - F_1(z_{0,out})) < 0, \\ \Leftrightarrow & \frac{F_1(z_0) - F_1(z_{0,out})}{F_1(z_{in}) - F_1(z_0)} < \frac{\omega \pi_1^{in}}{(1 - \omega) \pi_1^{out}} \end{aligned} \quad (13)$$

□

Condition 3.6 is generally true because our network detection algorithm (including the ‘quality and quantity criterions’) and permutation test ensure the communities have large proportions of highly correlated edges. We have run numerous empirical experiments and the results further verify this claim. If the assumption of network induced correlation matrix is true, the C selection procedure chooses the parameter to optimize the objective function of step one that reduce false positive findings and improve power simultaneously.

References

Banerjee, O., El Ghaoui, L. and d’Aspremont, A. (2008). Model selection through sparse maximum likelihood estimation for multivariate Gaussian or binary data. *The Journal of Machine Learning Research* **9**, 485-516.

- Besag, J., Kooperberg, C. (1995). On conditional and intrinsic autoregressions. *Biometrika*, **82**(4), 733-746.
- Bickel, P.J., Levina, E. (2008). Covariance regularization by thresholding. *Ann. Statist.* **36**, no. 6, 2577–2604.
- Bickel, P. J., Chen, A. (2009). A nonparametric view of network models and Newman-Girvan and other modularities. *Proceedings of the National Academy of Sciences*, **106**(50), 21068-21073.
- Bien, J., Bunea, F., Xiao, L. (2016). Convex banding of the covariance matrix. *Journal of the American Statistical Association*, 111(514), 834-845.
- Bonett, D. G., Price R. M. (2005). Inferential Methods for the Tetrachoric Correlation Coefficient. *Journal of Educational and Behavioral Statistics*, **30**, 213.
- Cai, T., Liu, W. and Luo, X. (2011). A constrained ℓ_1 minimization approach to sparse precision matrix estimation. *Journal of the American Statistical Association*, **106**, 594–607.
- Cai, T., Liu, W. (2011). Adaptive thresholding for sparse covariance matrix estimation. *J. Amer. Statist. Assoc.* **106** (494), 672–684.
- Cai, T. T., Ren, Z., Zhou, H. H. (2014). Estimating structured high-dimensional covariance and precision matrices: Optimal rates and adaptive estimation. *The Annals of Statistics*, **38**, 2118-2144.
- Chen, S., Li, M., Hong, D., Billheimer, D., Li, H., Xu, B. J., Shyr, Y. (2009). A novel comprehensive wave-form MS data processing method. *Bioinformatics*, **25**(6), 808-814.
- Chen, S., Kang, J., Wang, G. (2015). An empirical Bayes normalization method for connectivity metrics in resting state fMRI. *Frontiers in neuroscience*, **9**, 316-323.
- Chen, S., Kang, J., Xing, Y., Wang, G. (2015). A parsimonious statistical method to detect group-wise differentially expressed functional connectivity networks. *Human brain mapping*, **36**(12), 5196-5206.

- Chen, S., Bowman, F. D., Xing, Y. (2016). Differentially Expressed Functional Connectivity Networks with K-partite Graph Topology. arXiv preprint arXiv:1603.07211.
- Choi, D. S., Wolfe, P. J., Airoldi, E. M. (2012). Stochastic blockmodels with a growing number of classes. *Biometrika*, **99**, 273-284.
- Chung, F. R. (1997). Spectral Graph Theory (CBMS Regional Conference Series in Mathematics, No. 92), American Mathematical Society.
- Cui, Y., Leng, C., Sun, D. (2016). Sparse estimation of high-dimensional correlation matrices. *Computational Statistics & Data Analysis*, **93**, 390-403.
- Donoho, D. L., Johnstone, I. M., Kerkycharian, G. and Picard, D. (1995). Wavelet shrinkage: asymptopia? (with discussion). *Journal of the Royal Statistical Society, Series B* **57**, 301-369.
- Efron, B. (2004). Large-Scale Simultaneous Hypothesis Testing: The Choice of a Null Hypothesis. *Journal of the American Statistical Association*, **99**, 96-104.
- Efron, B. (2007). Size, power and false discovery rates. *The Annals of Statistics*, **35**(4), 1351-1377.
- Efron, B., Turnbull, B., Narasimhan, B. (2008). locfdr: Computes local false discovery rates. *R package*, 195.
- El Karoui, N. (2010). High-dimensionality effects in the markowitz problem and other quadratic programs with linear constraints: risk underestimation. *The Annals of Statistics*, **38**, 3487–3566.
- Fan, J., Liao, Y., Mincheva, M. (2013). Large covariance estimation by thresholding principal orthogonal complements. With 33 discussions by 57 authors and a reply by Fan, Liao and Mincheva. *J. R. Stat. Soc. Ser. B. Stat. Methodol.* **75**, no. 4, 603–680.
- Fan, J., Liao, Y., Liu, H. (2015). Estimating Large Covariance and Precision Matrices. arXiv preprint arXiv:1504.02995.
- Friedman, J., Hastie, T., Tibshirani, R. Sparse inverse covariance estimation with the graphical lasso. (2008). *Biostat.* **9**(3), 432–441.

- Friedman, J., Hastie, T., Tibshirani, R. (2010). Applications of the lasso and grouped lasso to the estimation of sparse graphical models (pp. 1-22). Technical report, Stanford University.
- Hsieh, C.J., Banerjee, A., Dhillon, I.S., Ravikumar, P.K.(2012) A divide-and-conquer method for sparse inverse covariance estimation *Advances in Neural Information Processing Systems* , 2330-2338
- Lam, C. and Fan, J. (2009). Sparsistency and rates of convergence in large covariance matrix estimation. *Annals of statistics* **37** 42-54.
- Lee, B. S., Jayathilaka, G. L. P., Huang, J. S., Vida, L. N., Honig, G. R., Gupta, S. (2011). Analyses of in vitro nonenzymatic glycation of normal and variant hemoglobins by MALDI-TOF mass spectrometry. *Journal of biomolecular techniques: JBT*, **22**(3), 90.
- Lei, J., Rinaldo, A. (2014). Consistency of spectral clustering in stochastic block models. *The Annals of Statistics*, **43**(1), 215-237.
- Liu, H., Wang, L. and Zhao, T. (2014). Sparse covariance matrix estimation with eigenvalue constraints. *Journal of Computational and Graphical Statistics*, **23**, 439-459.
- Jeffreys, H. (1961). *Theory of Probability*, 3rd ed. Clarendon Press, Oxford.
- Kass, R. E., Raftery, A. E. (1995). Bayes factors. *Journal of the american statistical association*, **90**(430), 773-795.
- Karrer, B., Newman, M. E. (2011). Stochastic block models and community structure in networks. *Physical Review E*, **83**(1), 016107.
- Kinney, J. B., Atwal, G. S. (2014). Equitability, mutual information, and the maximal information coefficient. *Proceedings of the National Academy of Sciences*, **111**(9), 3354-3359.
- Mazumder, R. and Hastie, T. (2012). Exact covariance thresholding into connected components for large-scale graphical lasso. *The Journal of Machine Learning Research*, **13**(1), 781-794.
- Nadakuditi, R. R., Newman, M. E. (2012). Graph spectra and the detectability of community structure in networks. *Physical review letters*, **108**(18), 188701.

- Rothman, A. J., Levina, E. and Zhu, J. (2009). Generalized thresholding of large covariance matrices. *Journal of the American Statistical Association* **104**, 177-186.
- Qi, H. and Sun, D. (2006). A quadratically convergent newton method for computing the nearest correlation matrix. *SIAM journal on matrix analysis and applications* **28** 360-385.
- Scott, J. G., Berger, J. O. (2006). An exploration of aspects of Bayesian multiple testing. *Journal of Statistical Planning and Inference*, **136**(7), 2144-2162.
- Scott, J. G., Berger, J. O. (2010). Bayes and empirical-Bayes multiplicity adjustment in the variable-selection problem. *The Annals of Statistics*, **38**(5), 2587-2619.
- Schäfer, J., Strimmer, K. (2005). A shrinkage approach to large-scale covariance matrix estimation and implications for functional genomics. *Statistical applications in genetics and molecular biology*, **4**(1).
- Shen, X., Pan, W. and Zhu, Y. (2012). Likelihood-based selection and sharp parameter estimation. *Journal of the American Statistical Association* **107** 223232.
- Shi, J., Malik, J. (2000). Normalized cuts and image segmentation. *Pattern Analysis and Machine Intelligence, IEEE Transactions on*, **22**(8), 888-905.
- von Luxburg, U. A tutorial on spectral clustering. (2007), *Stat. Comput.* **17** (4), 395–416.
- Tan, K. M., Witten, D., Shojaie, A. (2015). The cluster graphical lasso for improved estimation of Gaussian graphical models. *Computational statistics & data analysis*, **85**, 23-36.
- Witten, D. M., Friedman, J. H., Simon, N. (2011). New insights and faster computations for the graphical lasso. *Journal of Computational and Graphical Statistics*, **20**(4), 892-900.
- Wu, B., Guan, Z., Zhao, H. (2006). Parametric and nonparametric FDR estimation revisited. *Biometrics*, **62**(3), 735-744.
- Yildiz, P. B., Shyr, Y., Rahman, J. S., Wardwell, N. R., Zimmerman, L. J., Shakhtour, B., ... Massion, P. P. (2007). Diagnostic accuracy of MALDI mass spectrometric analysis of unfractionated serum in lung cancer. *Journal of thoracic oncology*, **2**(10), 893-915.

- Yuan, M. and Lin, Y. (2007). Model selection and estimation in the gaussian graphical model. *Biometrika*, **94**, 19–35.
- Yuan, M. (2010). High dimensional inverse covariance matrix estimation via linear programming. *Journal of Machine Learning Research*, **11**, 2261-2286.
- Zhang, C.-H. (2010). Nearly unbiased variable selection under minimax concave penalty. *The Annals of Statistics*, 894942.
- Zhao, Y., Levina, E., Zhu, J. (2011). Community extraction for social networks. *Proceedings of the National Academy of Sciences*, **108**(18), 7321-7326.